

Article (refereed) - postprint

Xu, Wen; Liu, Xuejun; Liu, Lei; Dore, Anthony J.; Tang, Aohan; Lu, Li; Wu, Qinghua; Zhang, Yangyang; Hao, Tianxiang; Pan, Yuepeng; Chen, Jianmin; Zhang, Fusuo. 2019. **Impact of emission controls on air quality in Beijing during APEC 2014: implications from water-soluble ions and carbonaceous aerosol in PM_{2.5} and their precursors.**

© 2019 Elsevier Ltd.

This manuscript version is made available under the CC-BY-NC-ND 4.0 license <http://creativecommons.org/licenses/by-nc-nd/4.0/>



This version available <http://nora.nerc.ac.uk/523091/>

NERC has developed NORA to enable users to access research outputs wholly or partially funded by NERC. Copyright and other rights for material on this site are retained by the rights owners. Users should read the terms and conditions of use of this material at <http://nora.nerc.ac.uk/policies.html#access>

NOTICE: this is an unedited manuscript accepted for publication. The manuscript will undergo copyediting, typesetting, and review of the resulting proof before publication in its final form. During the production process errors may be discovered which could affect the content. A definitive version was subsequently published in *Atmospheric Environment* (2019), 210, 241-252. <https://doi.org/10.1016/j.atmosenv.2019.04.050>

www.elsevier.com/

Contact CEH NORA team at
noraceh@ceh.ac.uk

1 MS Number: ATMENV-D-18-01742 R3

2

3 **Impact of emission controls on air quality in Beijing during APEC 2014:**
4 **Implications from water-soluble ions and carbonaceous aerosol in PM_{2.5} and**
5 **their precursors**

6

7 Wen Xu¹, Xuejun Liu^{1*}, Lei Liu², Anthony J. Dore³, Aohan Tang¹, Li Lu⁴, Qinghua
8 Wu¹, Yangyang Zhang¹, Tianxiang Hao¹, Yuepeng Pan⁵, Jianmin Chen⁶, Fusuo Zhang¹

9

10 ¹College of Resources and Environmental Sciences; National Academy of Agriculture Green
11 Development; Key Laboratory of Plant-Soil Interactions of MOE, China Agricultural University,
12 Beijing, 100193, China

13 ²International Institute for Earth System Science, Nanjing University, Nanjing, 210023, China

14 ³Centre for Ecology and Hydrology, Edinburgh, Bush Estate, Penicuik, Midlothian, EH26 0QB,
15 UK

16 ⁴Institute of Surface-Earth System Science, Tianjin University, Tianjin, 300072, China

17 ⁵State Key Laboratory of Atmospheric Boundary Layer Physics and Atmospheric Chemistry
18 (LAPC), Institute of Atmospheric Physics, Chinese Academy of Sciences, Beijing 100029, China

19 ⁶Department of Environmental Science and Engineering, Fudan University, Shanghai 200433,
20 China

21 *Correspondence to: X. J. Liu (liu310@cau.edu.cn); Tel: +86 10 62733459; Fax: +86 10 62731016

22

23

24

25

26

27

28

29

30

31

Abstract:

Stringent emission controls during the Asia Pacific Economic Cooperation Summit (APEC; November 5-11, 2014) provide a valuable opportunity to examine the impact of such measures on the chemical properties of $PM_{2.5}$ and other air pollutants. Here, we measured the water-soluble inorganic ions (WSII) and carbonaceous species in $PM_{2.5}$, NH_3 and NO_2 at multiple sites in Beijing between September and November 2014. Relative to the pre-APEC period (September and October 2014), significant reductions in the average concentrations of WSII (69% for NO_3^- , 68% for SO_4^{2-} , 78% for NH_4^+ , and 29-71% for other species), elemental carbon (EC, 43%) and organic carbon (OC, 45%) in $PM_{2.5}$ were found during the APEC period. The contributions of secondary inorganic ions (SIA, including SO_4^{2-} , NO_3^- , and NH_4^+) to $PM_{2.5}$ were significantly lower during the APEC period (9-44%), indicating a combination of lower gaseous precursor emissions and a relative weak secondary aerosol formation. Ion-balance calculations indicated that the $PM_{2.5}$ sample in the pre-APEC period was alkaline but was acidic during the APEC period. Relatively lower mean concentrations of EC ($1.5 \mu g m^{-3}$), OC ($10.5 \mu g m^{-3}$), secondary organic carbon (SOC, $3.3 \mu g m^{-3}$), secondary organic aerosol (SOA, $5.9 \mu g m^{-3}$) and primary organic aerosol (POA, $10.0 \mu g m^{-3}$) appeared during the APEC period. The average concentrations of NH_3 and NO_2 at all road sites were significantly reduced by 48 and 60% during the APEC period, which is consistent with clear reductions in satellite NH_3 columns over Beijing city in the same period. This finding suggests that reducing traffic emissions could be a feasible method to control urban NH_3 pollution. During the APEC period, concentrations of $PM_{2.5}$, PM_{10} , NO_2 , SO_2 and CO from the Beijing city monitoring network showed significant reductions at urban (20-60%) and rural (18-57%) sites, whereas O_3 concentrations increased significantly (by 93% and 53%, respectively). The control measures taken in the APEC period substantially decreased $PM_{2.5}$ pollution but can increase ground O_3 , which also merits attention.

Keywords: $PM_{2.5}$, Ammonia, Chemical components, Air pollution, Emission control

60

61

62 1. Introduction

63 Over recent decades, Beijing, the capital of China, has experienced severe air
64 pollution caused mainly by a growth in energy consumption and associated
65 multipollutant emissions (Zhang et al., 2016a). Of particular concern is PM_{2.5}
66 (particulate matter ≤ 2.5 μm in aerodynamic diameter) pollution, which has adverse
67 influences on human health (Cohen et al., 2017; Gu and Yim, 2016) and climate
68 change (Kaufman et al., 2002; Koren et al., 2014; Guo et al., 2016; 2017), as well as
69 the eco-environment (Li et al., 2017; Yue et al., 2017). Increasing concern about haze
70 pollution has recently motivated studies focusing on the sources and formation
71 mechanisms of PM_{2.5} in China (Ma et al., 2018; Wang et al., 2018; Zhang et al., 2018).
72 However, the sources and formation mechanisms of atmospheric PM_{2.5} are less well
73 known and differ from region to region (Liu et al., 2017a). Based on the analysis of
74 chemical components in PM_{2.5}, the latest results released from Beijing's
75 Environmental Protection Bureau
76 ([http://www.bjepb.gov.cn/bjhrb/xxgk/jgzl/jgsz/jjgigszjzz/xcyj/xwfb/832588/index.ht](http://www.bjepb.gov.cn/bjhrb/xxgk/jgzl/jgsz/jjgigszjzz/xcyj/xwfb/832588/index.html)
77 [ml](http://www.bjepb.gov.cn/bjhrb/xxgk/jgzl/jgsz/jjgigszjzz/xcyj/xwfb/832588/index.html)) showed that two-thirds of Beijing's PM_{2.5} originated from local emissions, of
78 which the four major contributors were motor vehicles (45%), fugitive dust (16%),
79 industrial production (12%), and household emissions (12%). The remaining emission
80 sources (15%) were derived from coal combustion (3%) and agricultural and natural
81 sources (12%). Hence, detailed investigations of the chemical and physical properties
82 of PM_{2.5} promote an understanding of their sources and formation processes (Huang
83 et al., 2014; Han et al., 2016).

84 Water-soluble inorganic ions (WSII) are the main chemical components of PM_{2.5}.
85 Sulfate, nitrate, and ammonium (i.e., secondary inorganic aerosol, abbreviated as SIA)
86 collectively account for approximately 29% of the PM_{2.5} mass in Beijing in
87 2012-2014 (Xu et al., 2016a). During the extremely severe and persistent haze
88 episodes in January 2013, the contribution of SIA to PM_{2.5} was approximately 37%
89 (Huang et al., 2014). Secondary inorganic aerosol exacerbated haze development as
90 reflected by their increased contributions during haze episodes (Sun et al., 2014). By
91 contrast, during summer months WSII accounted for 60% of the PM_{2.5} mass in

92 Beijing with highly acidic $PM_{2.5}$ observed during haze pollution (Zhang et al., 2016b).
93 In addition, carbonaceous aerosols are also important components of $PM_{2.5}$ and
94 comprise elemental carbon (EC) and organic carbon (OC). EC is exclusively emitted
95 as primary aerosols from incomplete combustion of fossil fuels and biomass burning,
96 whereas OC is a complex mixture of primary directly emitted OC particles (POC) and
97 secondary OC (SOC) formed in the atmosphere via the oxidation of gas-phase
98 precursors (e.g., volatile organic compounds, VOCs). Common sources of
99 atmospheric POC and of SOC precursors include vehicular exhaust, coal combustion,
100 cooking, biogenic emissions, and biomass burning (Pöschl, 2005; Zhao et al., 2013).
101 During the cold season in Beijing, fossil emissions from coal combustion contributed
102 33% of EC with the remainder from vehicle exhaust, whereas. In warm periods,
103 greater than 90% of fossil EC was associated with vehicle emissions (Zhang et al.,
104 2015a). In addition to fossil emission, non-fossil emission was also a very important
105 contributor of carbonaceous aerosol in urban Beijing with the contributions from
106 biomass burning of 25% and 48% for EC and OC, respectively (Zhang et al., 2015b).
107 Therefore, investigation of the chemical components of $PM_{2.5}$ could provide useful
108 insights into the sources and chemical and physical reaction mechanisms leading to
109 the formation of haze in Beijing.

110 Stringent emission controls to reduce levels of air pollution have been proven to
111 temporally improve air quality during specific events in Beijing, such as the 2008
112 Beijing Olympic Games (Shen et al., 2011; Schleicher et al., 2012), the 2014
113 Asia-Pacific Economy Cooperation (APEC) China Summit (Wang et al., 2016), and
114 the 2015 China Victory Day Parade (Xu et al., 2017). For example, for the 2014
115 APEC Summit, a series of stringent measures were enforced in Beijing and the
116 surrounding regions in northern China from 3-12 November to ensure good air quality
117 during the APEC summit in Beijing. The specific measures include the following: 1)
118 restrictions on the days when vehicle usage was permitted according to the
119 registration plate (odd or even number); 2) a one-week delay in the start of the winter
120 heating season; 3) coal-fueled industries were suspended or had restricted operations;
121 4) construction sites were closed (Liu et al., 2017b). Owing to such emission controls,

122 concentrations of sulfur dioxide (SO₂), nitrogen oxides (NO_x), PM₁₀ (particulate
123 matter < 10 μm), PM_{2.5} and VOCs emissions decreased by 33.6-66.6% (BMEPB,
124 2014). During the APEC weeklong meeting, blue-sky days with good air quality were
125 frequently observed in Beijing, which has been called the “APEC Blue” period.

126 To date, some studies have focused on chemical composition, size distribution,
127 oxidation properties, and precursors of submicron aerosol (PM₁) before, during and
128 after the APEC summit (e.g., Chen et al., 2015; Sun et al., 2016). A recent study
129 reported that the concentrations of PM_{2.5} and associated chemical components
130 decreased significantly at a rural site in Beijing during the APEC period (Wang et al.,
131 2017). However, few previous studies have paid attention to the chemical variations
132 and formation cause of PM_{2.5} during control and no control periods in the urban
133 Beijing environment. Although the traffic as a major contributor of atmospheric NH₃
134 in Beijing was initially reported by Ianniello et al. (2010) and later by Chang et al.
135 (2016) and Xu et al. (2017), it remains unclear whether a reduction of on-road
136 vehicles can significantly lower atmospheric NH₃ levels over Beijing. This question is
137 worthy of exploration by synchronous analysis of NH₃ concentrations measured at
138 road sites and from space observations. Satellite NH₃ observations have been recently
139 used to diagnose NH₃ emission dynamics (Liu et al., 2017c).

140 From a policy perspective, it is desirable to study the effect that implementing
141 controls on pollutant emissions has on the chemical properties of PM_{2.5} as well as its
142 gaseous precursors (e.g., NH₃, SO₂, NO₂), because this knowledge is necessary to
143 guide future pollution control strategies. Therefore, the objective of this research was
144 to evaluate the effectiveness of pollution control measures on air quality improvement
145 in Beijing through measurements of WSII and carbonaceous compounds in PM_{2.5}
146 from urban Beijing, NH₃ and NO₂ concentrations from road sites of Beijing and the
147 daily mean concentrations of PM_{2.5}, PM₁₀, NO₂, SO₂, CO and O₃ across Beijing
148 before and during the APEC period.

149 **2. Materials and methods**

150 *2.1. Sampling site and sample collection*

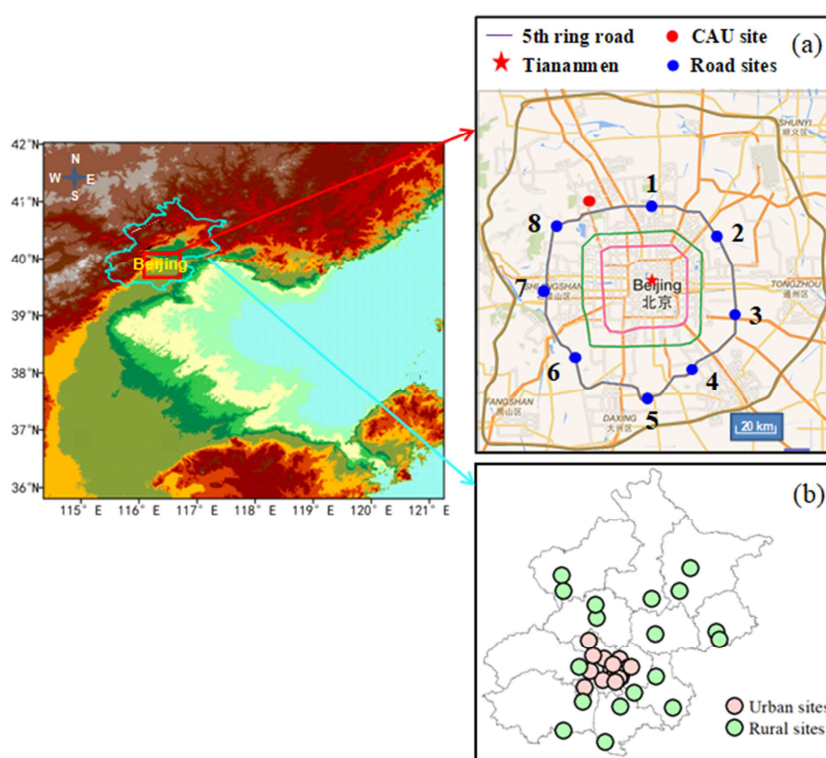
151 The sampling site of airborne PM_{2.5} was located on the roof of the Resource and

152 Environment building (~15 m above the ground) at west campus of China
153 Agricultural University (CAU, 40.02° N, 116.28° E, 55 m a.s.l.) which is 16.8 km
154 northwest of Tiananmen Square in the city center (**Fig. 1a**). The site was located in a
155 region with educational, commercial, and residential areas in the local vicinity as well
156 as traffic sources. No large pollution sources are present around the sampling sites.
157 Thus, our observation site can be considered representative of the urban environment.
158 Daily PM_{2.5} samples (from 8:00 am to 8:00 am next day) were collected from 20 to 31
159 October (named the pre-APEC period, excluding 21 and 25 October due to instrument
160 failure) and from 3 to 12 November 2014 (named APEC period) on 90-mm quartz
161 fiber filters (Whatman QM/A, Maidstone, UK) using medium-volume air samplers
162 (TH-150C, Tianhong Instruments Co., Wuhan, China). The flow rate was set at 100 L
163 min⁻¹. All quartz filters were prebaked at 500°C for 4 h to remove residual carbon
164 species. The filters were wrapped in aluminum foil after sampling and stored at -20°C
165 before analysis to prevent the evaporation of volatile components.

166 Gaseous NH₃ and NO₂ samples were collected from 24 to 28 September, 23 to
167 30 October, and 3 to 13 November 2014 (i.e., with a duration of 5-11 days) at eight
168 road sites, which were evenly distributed at the edges of the fifth ring road (**Fig. 1a**).
169 NH₃ samples were collected using ALPHA passive samplers (Tang et al., 2001) and
170 NO₂ samples were collected using Gradko diffusion tubes (Gradko International
171 Limited, UK). The ALPHA sampler used a citric acid coated filter to capture NH₃,
172 while Gradko tubes used 20% triethanolamine/deionized water solution-coated
173 stainless steel wire mesh to capture NO₂. For the two types of samplers, detection
174 limits are 0.12 µg NH₃ m⁻³ and 1.6 µg NO₂ m⁻³ (Puchalski et al., 2011). At all sites,
175 three ALPHA and three Gradko samplers were exposed under a PVC shelter at
176 approximately 1.5 m height above ground. **Fig. S1** in the supplementary material
177 illustrates two road sites.

178 After sampling, all samples were returned to the laboratory and stored at 4°C
179 prior to chemical analysis. At each site, three field (travel) blank filters were prepared
180 to assess background contamination from the field. In addition, three laboratory blank
181 filters were stored in a clean desiccator at room temperature for assessing background

182 contamination from the laboratory.



183

184 **Fig. 1.** Maps showing the monitoring area (left Figure), monitoring sites in urban
 185 Beijing (red and blue points represent CAU site and 8 road sites on the fifth ring road,
 186 respectively) (a) and the surrounding regions (b). The location of Tiananmen (red
 187 five-pointed star) is also shown (a).

188 2.2. Analytical procedures

189 PM_{2.5} mass concentrations were analyzed gravimetrically using an electronic
 190 microbalance (sensitivity: $\pm 10 \mu\text{g}$, Sartorius, Gottingen, Germany). The blank and
 191 sample filters were equilibrated at a temperature of 20–25°C and relative humidity of
 192 35–45% for 24 h before and after sampling. A 1/4 piece of collected PM_{2.5} samples
 193 was put into a glass tube (60 mL) and was ultrasonically extracted with 10 mL
 194 high-purity water (18.2 M Ω) for 30 min. The extracts were then filtered through 0.22
 195 mm PTFE syringe filter to remove insoluble matters. Five cations (NH₄⁺, Na⁺, K⁺,
 196 Mg²⁺, and Ca²⁺) and four anions (SO₄²⁻, NO₃⁻, F⁻, and Cl⁻) in the filtrates were
 197 determined using Dionex-600 and Dionex-2100 Ion Chromatograph (Dionex Inc.,
 198 Sunnyvale, CA, USA), respectively, with detection limits of 0.01–0.02 mg L⁻¹ for the
 199 measured ions (Zhang et al., 2011; Tao et al., 2014).

200 A 0.5 cm² punch from each quartz fiber filter was analyzed for organic carbon
201 (OC) and elemental carbon (EC) using a Desert Research Institute (DRI) Model 2001
202 Thermal/Optical Carbon Analyzer (Atmoslytic Inc., Calabasas, CA, USA) with
203 IMPROVE_A (Interagency Monitoring of Protected Visual Environment)
204 thermal/optical reflectance (TOR) protocol (Chow et al., 2007).

205 The NH₃ filters, extracted with 10 mL high-purity water, were determined using
206 a continuous-flow analyzer (Seal AA3, Germany). The NO₂ samples were extracted
207 with a solution containing sulfanilamide, H₃PO₄ and N-1-Naphthylethylene-diamine,
208 and measured using a colorimetric method by absorption at a wavelength of 542 nm.

209 The field (travel) and laboratory blanks were extracted and analyzed using the
210 same methods as the exposed samples. All reported concentrations of NH₃, NO₂, and
211 PM_{2.5} and its associated chemical components were corrected for the blanks.

212 2.3. Estimation of secondary organic aerosol concentrations

213 Organic carbon can be divided into SOC and POC. The SOC content in PM_{2.5}
214 was estimated by determining POC concentration using EC as a tracer and then
215 subtracting the POC from the measured total OC. The primary organic aerosol (POA)
216 concentration was calculated as the product of POC and the ratio of OM to OC in the
217 POA (OM/OC_{POA}). The equations for these calculations are shown as follows (Xu et
218 al., 2015):

$$219 \quad \text{POC} = \text{EC} \times (\text{OC}/\text{EC})_{\text{primary}} \quad (1)$$

$$220 \quad \text{SOC} = \text{OC} - \text{POC} \quad (2)$$

$$221 \quad \text{POA} = \text{POC} \times (\text{OM}/\text{OC}_{\text{POA}}) \quad (3)$$

222 where (OC/EC)_{primary} is the estimated primary carbon ratio, the minimum ratio of
223 OC/EC was taken as representative of (OC/EC)_{primary} (Pant et al., 2015; Dai et al.,
224 2018), and OC above that ratio was taken to be SOC. As reported by previous studies
225 (Xu et al., 2014; Zhang et al., 2014), the OM/OC ratio for fresh urban organics in
226 northern China was between 1.2 and 1.6. Since it is expected that oxidation of organic
227 aerosols can occur during transport, we used the ratio of 1.4 for the OM/OC_{POA},
228 consistent with the study of Dai et al. (2018). The secondary organic carbon (SOA)
229 was calculated by multiplying SOC by a coefficient of 1.8 (Philip et al., 2014).

230 *2.4. Data of major air pollutants, satellite NH₃ columns, and meteorological*
231 *parameters*

232 Comparison of the major air pollutants between the pre-APEC and APEC
233 periods were evaluated at a city level in Beijing. The 24 h average concentrations of
234 PM_{2.5}, PM₁₀, NO₂, SO₂, CO and O₃ measured at 35 sites across Beijing (17 urban and
235 18 rural sites, **Fig. 1b**) were downloaded from Beijing Municipal Environmental
236 Monitoring Center (<http://www.bjmemc.com.cn/>). For NH₃, we used the new
237 IASI_NH₃ columns product (downloaded from the Atmospheric Spectroscopy Group
238 at Université Libre De Bruxelles, <http://www.ulb.ac.be/cpm/atmosphere.html>) as the
239 Artificial Neural Network for IASI ANNI-NH3-v2.1R-I (Van Damme et al. 2017),
240 which is based on ERA-Interim ECMWF meteorological input data. The IASI_NH₃
241 observations have an elliptical footprint which covers a variable area between 12 and
242 12 km up to 20 by 39 km depending on the satellite-viewing angle. We then processed
243 the data into a 0.25° latitude × 0.25° longitude gridded map by averaging the daily
244 values with observations points within the grid cell over the specific time periods (Liu
245 et al., 2017c). Daily meteorological data, including wind direction, wind speed, air
246 temperature, relative humidity and atmospheric pressure during the pre-APEC and
247 APEC periods were observed using an automatic meteorological observation
248 instrument (Milos520, Vaisala, Finland).

249 *2.5. Back trajectories*

250 Backward trajectories arriving at Beijing were calculated using the Hybrid Single
251 Particle Lagrangian Integrated Trajectory (HYSPLIT4) from NOAA 4.9 model
252 (<http://www.arl.noaa.gov/ready/open/hysplit4.html>). The trajectories were run for a
253 72h time period and initialized from a 500 m height at 6 h intervals (00:00, 06:00,
254 12:00 and 18:00 UTC) each day. The trajectories were classified into several types
255 using cluster analysis based on the total spatial variance (TSV) method (Draxler et al.,
256 2012).

257 *2.6. Statistical analysis*

258 The two independent samples t tests were employed to examine temporal
259 differences between study phases for investigated variables, including concentrations

260 of NH_3 and NO_2 at road sites, $\text{PM}_{2.5}$ and its chemical components at the CAU site, and
261 open-accessed pollutants (i.e. $\text{PM}_{2.5}$, PM_{10} , NO_2 , SO_2 , CO and O_3). All statistical
262 analyses were conducted using SPSS11.5 (SPSS Inc., Chicago, IL, USA), and
263 significance was set at $p < 0.05$. The concentrations of all measured variables per
264 sampling period at the sampling sites are presented as the mean \pm standard deviation.

265 **3. Results and discussion**

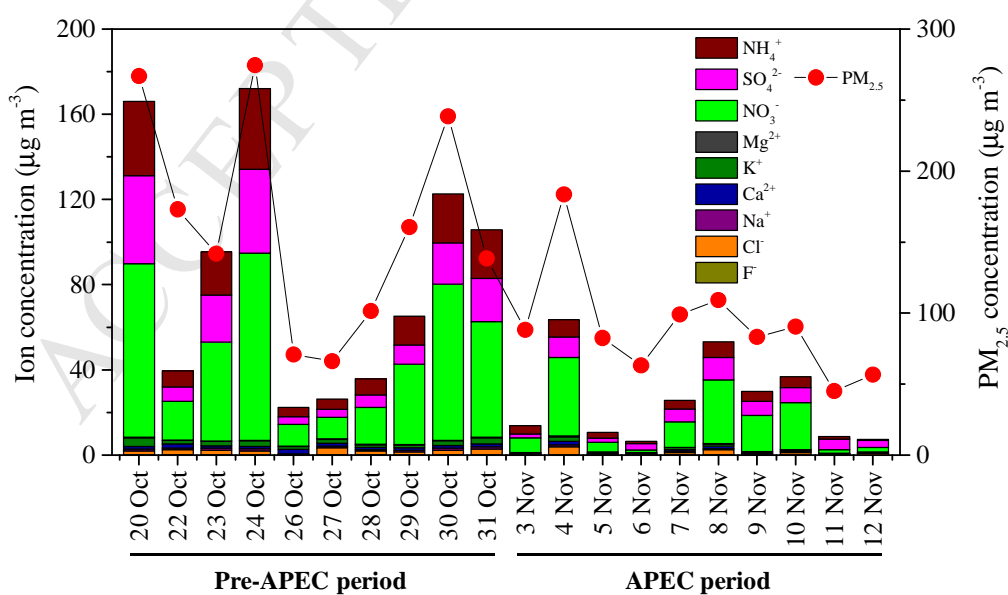
266 *3.1. Characteristics of $\text{PM}_{2.5}$ and other pollutants*

267 Daily $\text{PM}_{2.5}$ concentrations at the CAU site ranged from 45.0 to 274.5 $\mu\text{g m}^{-3}$
268 during the entire sampling period, with a mean value of $126.7 \pm 69.5 \mu\text{g m}^{-3}$ (**Fig. 2**).
269 The average concentration of $\text{PM}_{2.5}$ during the APEC period ($90.1 \pm 38.3 \mu\text{g m}^{-3}$) was
270 45% lower ($p < 0.05$) than the mean during the pre-APEC period ($163.2 \pm 75.8 \mu\text{g m}^{-3}$).
271 Emission control measures and meteorology alternated to modulate $\text{PM}_{2.5}$ during the
272 APEC period with the latter dominating the absolute reduction of $\text{PM}_{2.5}$ (Gao et al.,
273 2017; Liu et al., 2017b). A similar study (Xu et al., 2017) revealed that compared with
274 the effect of meteorological conditions, the emission control measures played a
275 dominant role in $\text{PM}_{2.5}$ mitigation during the Parade Blue period in Beijing. Average
276 $\text{PM}_{2.5}$ concentration during the APEC period was approximately 10% lower than the
277 average of $100 \mu\text{g m}^{-3}$ observed during an autumn episode of 2011 in the Yangtze
278 River Delta (Hua et al., 2015) but approximately 60% higher than the averages
279 reported during the Olympic and Parade Blue periods (40.1 and $37.2 \mu\text{g m}^{-3}$,
280 respectively) in urban areas of Beijing (Shen et al., 2011; Xu et al., 2017). Compared
281 with the Olympic and Parade Blue periods when favorable meteorological conditions
282 (e.g., more precipitation and higher mixing layer height) resulted in lowering $\text{PM}_{2.5}$
283 concentrations occurred (Xu et al., 2017), the APEC summit was held in the middle of
284 November with unfavorable meteorological conditions (e.g., no precipitation, stable
285 atmospheric pressure, and relatively low wind speed, **Fig. 3**), which to some extent
286 led to relatively higher $\text{PM}_{2.5}$ concentrations.

287 It should be noted that the meteorological parameters analyzed in this study were
288 obtained from near surface measurements, which have certain limitations. It is too
289 hard to determine the haze formation mechanism without considering the vertical

290 stratification, such as the planetary boundary layer (PBL) and temperature inversion
 291 (TI). For example, the PBL is inherently associated with air pollution as the bulk of
 292 aerosols reside in the PBL, and the strong interactions or feedbacks between aerosols
 293 and the PBL (Yu et al., 2002). These interactions can greatly exacerbate air pollution,
 294 even if emission rates remain unchanged. Surface dimming (by all types of aerosols)
 295 and upper-PBL warming (by absorbing aerosols) help stabilize the PBL and weaken
 296 turbulence mixing, resulting in a decrease in the boundary-layer height, which
 297 subsequently favors the accumulation of air pollutants in a shallower PBL (Ding et al.,
 298 2016; Petäjä et al., 2016). In addition, the absorption of solar radiation by aerosols can
 299 induce a TI at the top of the PBL which is often related to severe pollution episodes
 300 (Li et al., 2017). Generally, high concentrations of aerosols and gaseous pollutants
 301 (e.g., SO₂ and NO₂) occurred in the atmosphere in the presence of a TI.

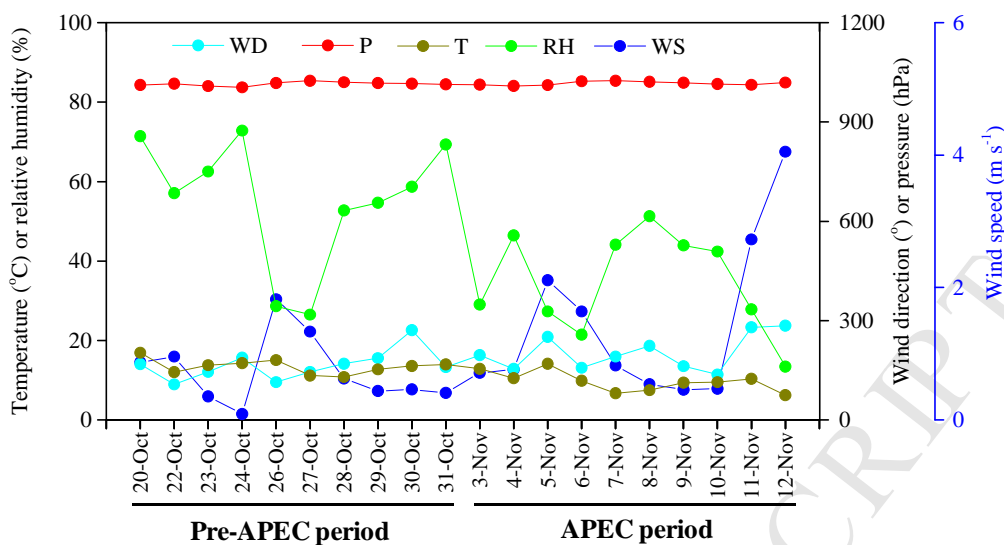
302 Although stringent emission control measures were enforced, PM_{2.5}
 303 concentration reached 183.6 µg m⁻³ on 4 November. The main explanation for this
 304 observation is that the air masses from westerly and southwesterly directions (i.e.,
 305 aerosol pollution source region) of Beijing led to high concentrations of PM_{2.5} and its
 306 gaseous precursors (NH₃, NO_x and SO₂) (Fig. S2).



307

308 **Fig. 2.** Concentrations of PM_{2.5} and associated water-soluble ions at the CAU site.

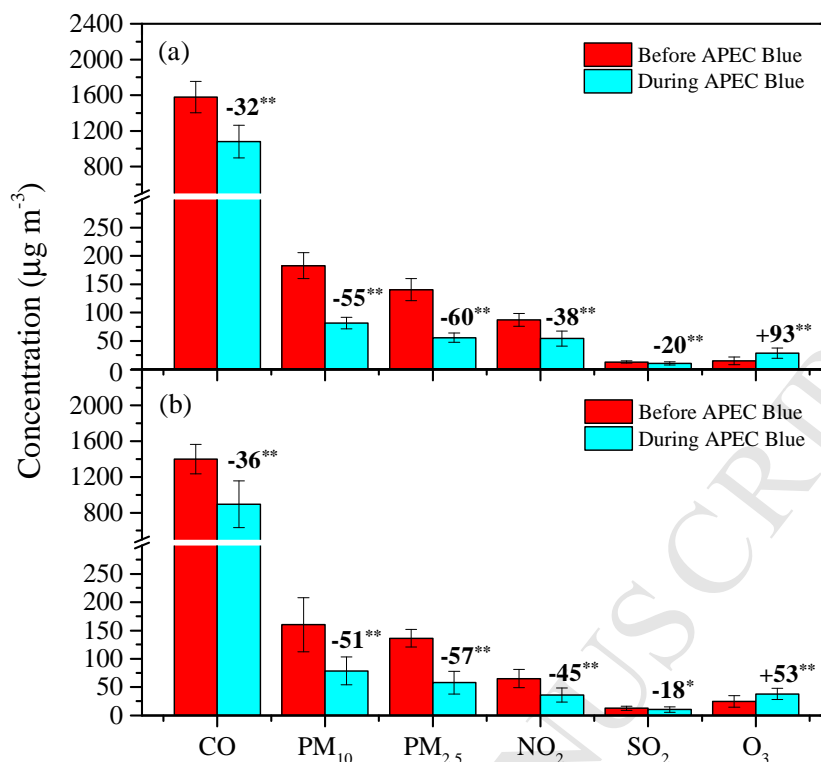
309



310

311 **Fig. 3.** Temporal variations in daily wind direction (WD), wind speed (WS), air
 312 temperature (T), relative humidity (RH) and atmospheric pressure (P) during the
 313 pre-APEC and APEC periods in Beijing.

314 Daily average concentrations of the six major pollutants (PM_{2.5}, PM₁₀, NO₂, SO₂,
 315 CO and O₃) in Beijing were averaged for 17 urban sites and 18 rural sites (**Fig. 1**), as
 316 shown in **Fig. 4a and b**. Concentrations of PM_{2.5}, PM₁₀, NO₂, SO₂ and CO at all sites
 317 showed highly significant ($p < 0.01$) decreases (by 20-60% and 18-57%, respectively)
 318 during the APEC period compared with the pre-APEC period, demonstrating a strong
 319 beneficial effect of emission control measures. However, the mean O₃ concentrations
 320 were significantly higher in the APEC period than in the pre-APEC period. This
 321 phenomenon could be explained by the fact that the lower concentrations of primary
 322 pollutants (i.e., NO_x=NO+NO₂) during the APEC period led to a lower efficiency of
 323 O₃ destructions as the major destruction mechanism for O₃ is the oxidation of nitric
 324 oxide (NO) to form NO₂ (Paschalidou and Kassomenos, 2004). In addition, a rapid
 325 decrease of PM_{2.5} can slow down the sink of hydroperoxy radicals and thus speeded
 326 up O₃ production, resulting in high atmospheric O₃ concentrations (Li et al., 2019).



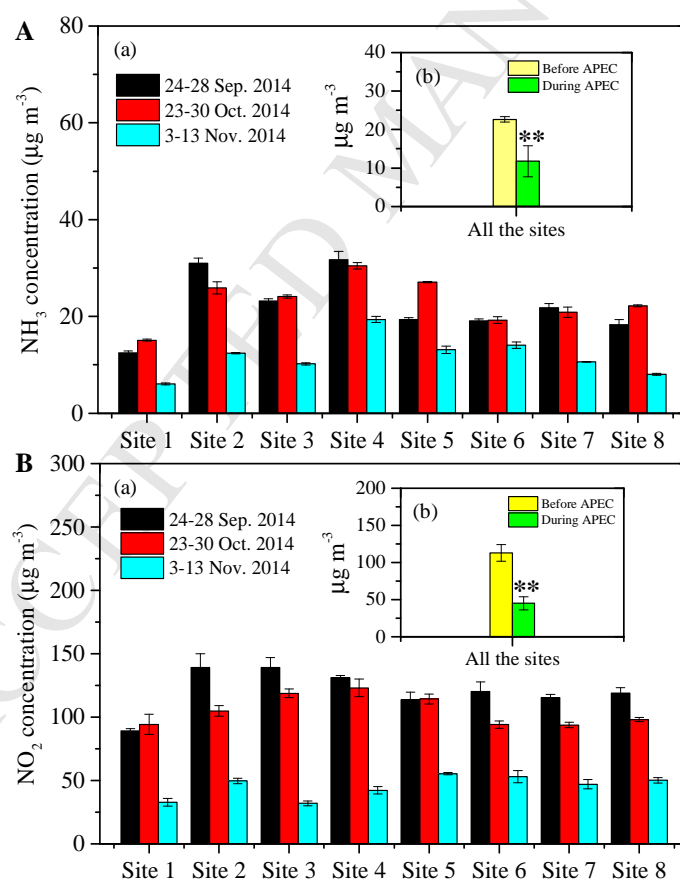
327

328 **Fig. 4.** Comparison of average concentrations of PM_{2.5}, PM₁₀, NO₂, SO₂ and CO
 329 between the pre-APEC and APEC periods for 17 urban sites (a) and 18 rural sites (b)
 330 in Beijing. The error bars are the standard deviations of means. Negative and positive
 331 values on the bar represent decreases and increases (in percentage), respectively. * and
 332 ** the mean significance at the 0.05 and 0.01 probability levels for the difference in
 333 mean concentrations of each pollutant between the pre-APEC and APEC periods,
 334 respectively, at rural or urban sites.

335

336 The NH₃ concentrations at the eight road sites were 12.5-31.7, 15.1-30.5, and
 337 6.1-19.4 µg m⁻³ for 24-28 September, 23-30 October, and 3-13 November,
 338 respectively (**Fig. 5A, panel a**). Correspondingly, the NO₂ concentrations were
 339 89.0-139.2, 93.7-123.0, and 31.8-55.3 µg m⁻³, respectively (**Fig. 5B, panel a**). Across
 340 all the sites, average concentrations of NH₃ and NO₂ during the APEC period (11.7 ±
 341 4.1 and 45.2 ± 8.9 µg m⁻³, respectively) were 48% and 60% lower (*p*<0.01),
 342 respectively, than the corresponding means during the pre-APEC period (**Fig. 5A and**
 343 **B, panel b**). The measured NH₃ concentrations for 23-30 October were 2.3 times the
 344 ambient mean value of 9.9 µg m⁻³ measured during a similar period at the urban site

345 in Beijing (Chang et al., 2016). These results demonstrated that traffic is a significant
 346 source of NH_3 concentrations in urban Beijing. From satellite observations (**Fig. 6a**),
 347 the IASI_ NH_3 columns were comparable between the two subperiods (i.e., 24-28
 348 September and 23-30 October) within the pre-APEC period over Beijing city, and
 349 both were clearly higher than the values observed during the APEC period (i.e., 3-13
 350 November). The difference in IASI_ NH_3 columns during different time periods was
 351 $-2.43 \times 10^5 \text{ molec cm}^{-3}$ between 3-13 November and 24-28 September, and -3.18×10^5
 352 molec cm^{-3} between 3-13 November and 23-30 October (**Fig. 6b**). Our results suggest
 353 that reducing traffic vehicle numbers could lower ambient NH_3 concentration at a city
 354 level. In addition, reducing urban NH_3 emission could be an effective method for
 355 reducing the formation of secondary inorganic $\text{PM}_{2.5}$ pollution in Beijing (Xu et al.,
 356 2017).



357

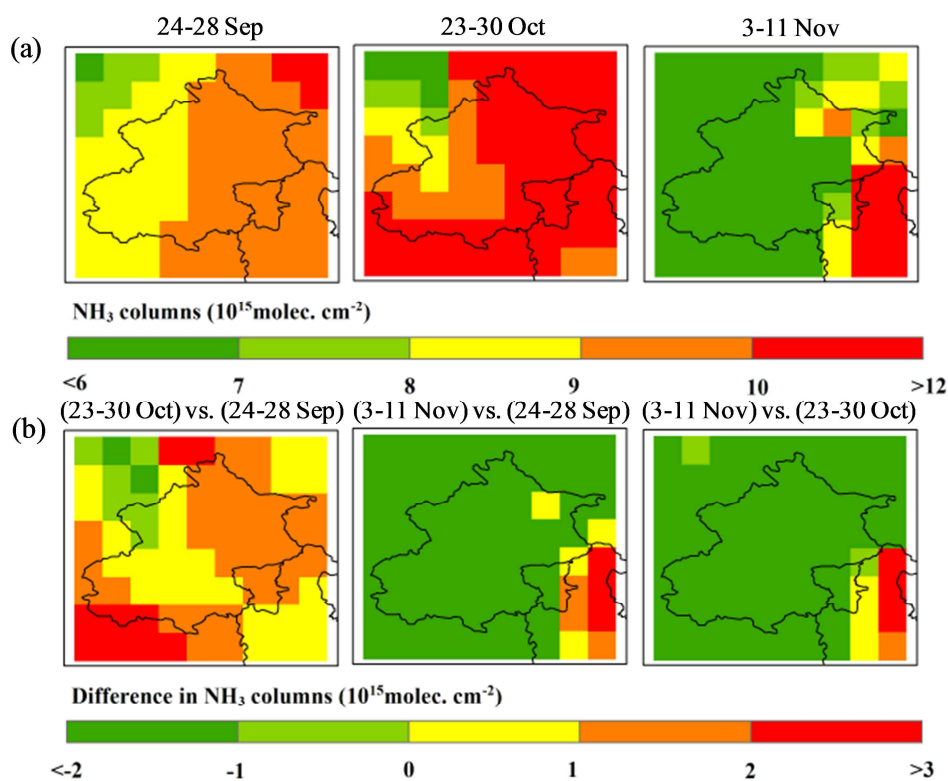
358 **Fig. 5.** Concentrations of NH_3 (A) and NO_2 (B) during the sampling periods at

359 different observation scales: concentrations at 8 road sites (a) and averaged

360 concentrations for the sites (b). Values before the APEC period (i.e., yellow bar) were

361 averaged from those in the periods of 24-28 September and 23-30 October 2014. The
 362 error bars are the standard deviations of means. Two asterisks on bars indicate
 363 significant difference at $p < 0.01$.

364



365

366 **Fig. 6.** Average IASI_NH₃ columns over Beijing city and its surrounding areas during
 367 the periods of 24-28 September 2014, 23-30 October 2014, and 3-13 November 2014
 368 (a), and the difference of IASI_NH₃ columns between the three time periods (b).

369

370 3.2. Water-soluble inorganic ions in PM_{2.5}

371 Time series and the averages of daily WSII concentrations in PM_{2.5} are presented
 372 in **Fig. 2** and **Table 1**. The average concentrations of total water-soluble inorganic
 373 ions (TWSII) ranged from 6.5 to 171.8 $\mu\text{g m}^{-3}$, with a significant ($p < 0.05$) reduction
 374 (70%) in the mean observed during the APEC period compared with the pre-APEC
 375 period (25.62 ± 20.25 vs. 85.07 ± 56.13 $\mu\text{g m}^{-3}$). SO₄²⁻, NO₃⁻, and NH₄⁺ are the
 376 predominant ions in PM_{2.5} and collectively accounted for 71-96% (average 88%) of
 377 TWSII and for 9-70% (34%) of PM_{2.5} mass concentration (**Fig. 2**). The concentrations

378 of SO_4^{2-} , NO_3^- , and NH_4^+ during the APEC period were in the ranges of 1.8-10.5,
 379 1.2-36.7, and 0.4-8.1 $\mu\text{g m}^{-3}$, respectively (**Fig. 2**); the means of which were all
 380 significantly ($p<0.05$) lower (by 68%, 69% and 78%, respectively) than those in the
 381 pre-APEC period (**Table 1**). By contrast, the daily concentrations of other ions (i.e.,
 382 Ca^{2+} , K^+ , Na^+ , Mg^{2+} and F^-) during the APEC period were overall within the range of
 383 0.01-4.12 $\mu\text{g m}^{-3}$ (**Fig. 2**) and showed significant reductions (29-71%), except for Cl^-
 384 (**Table 1**).

385

386 **Table 1.** Comparison of mean (standard deviation) concentrations ($\mu\text{g m}^{-3}$) of $\text{PM}_{2.5}$
 387 and associated water-soluble inorganic ions between urban and rural sites in Beijing.

	Urban site in Beijing (this study)				Rural site in Beijing ^a			
	Entire (N=20)	Before (N=10)	During (N=10)	Reduction (%)	Entire (N=24)	Before (N=12)	During (N=12)	Reduction (%)
$\text{PM}_{2.5}$	126.67 (69.46)	163.24 (75.84)	90.10 (38.25)	45*	79.3	115.5	39.9	65
NO_3^-	28.56 (27.17)	43.70 (29.82)	13.43 (12.67)	69**	14.9	23.3	6.6	72
SO_4^{2-}	11.30 (11.55)	17.10 (14.06)	5.49 (3.05)	68*	9.8	14.2	4.3	70
NH_4^+	10.76 (11.12)	17.66 (12.19)	3.87 (2.59)	78**	7.9	12.8	2.8	78
Ca^{2+}	0.93 (0.60)	1.34 (0.33)	0.51 (0.52)	62**	1.1	1.3	0.5	62
K^+	1.37 (1.08)	2.12 (0.88)	0.62 (0.65)	71**	1.0	1.2	0.6	50
F^-	0.06 (0.02)	0.07 (0.02)	0.05 (0.02)	29*	n.a.	n.a.	n.a.	n.a.
Cl^-	1.57 (1.09)	2.02 (0.84)	1.13 (1.17)	44	1.3	1.4	0.7	50
Na^+	0.60 (0.33)	0.83 (0.26)	0.38 (0.22)	54**	0.2	0.2	0.2	
Mg^{2+}	0.19 (0.10)	0.24 (0.04)	0.14 (0.12)	40*	0.2	0.2	0.1	50
OC	13.92 (6.49)	18.86 (4.32)	10.46 (5.49)	45**	13.7	18.2	6.9	62
EC	1.91 (0.92)	2.55 (0.22)	1.45 (0.97)	43**	3.7	5.2	1.7	67

388 N: number; n.a. denotes that the data was not available

389 ^aData from Wang et al. (2017)

390 * and ** mean significance at the 0.05 and 0.01 probability levels for the difference in
391 mean concentrations of PM_{2.5} and associated components between the pre-APEC and
392 APEC Blue periods, respectively.

393

394 Compared with the rural site in the Huairou district of Beijing (**Table 1**), the
395 average concentrations of PM_{2.5} and NO₃⁻ in the present study were overall 41-126%
396 higher during the pre-APEC and APEC periods, whereas comparable concentration
397 levels were observed for remaining WSII. In addition, the concentrations of PM_{2.5} and
398 individual WSII species showed similar reductions in magnitude. The WSII
399 concentrations in PM_{2.5} in Beijing during the APEC period were generally lower than
400 those measured in all eight provincial capital cities, except the NO₃⁻ concentration
401 (19-163% higher than those observed in Shenzhen, Chengdu, Lanzhou, Guangzhou
402 and Wuhan cities) (**Table 2**). However, regarding SIA, NO₃⁻ concentrations during the
403 APEC period were higher than those observed at all urban sites around the world,
404 whereas the concentrations of SO₄²⁻ and NH₄⁺ were generally at slightly higher or
405 comparable levels (**Table 3**).

406

407

408

409

410

411

412

413

414

415

416

417

418

419

420

421

422

423

424 **Table 2.** Comparison of the concentrations (mean \pm SD) of water-soluble inorganic ions in Beijing with other cities in China.

	Beijing APEC period This study	Xi'an, Jan-Feb, 2010 ^a	Shanghai, Sep-Nov, 2013 ^b	Shenzhen, Nov-Dec, 2009-2010 ^c	Chengdu, 2014-2016 ^d	Lanzhou, Dec. 2013 ^e	Guangzhou Jan-Dec, 2013 ^f	Wuhan Jan-Dec, 2013 ^g	Zhengzhou Autumn, 2014 ^h
N	10	56	16	61	210	31	169	52	14
NO ₃ ⁻	13.4 \pm 12.7	22.9 \pm 17.4	15.0 \pm 18.2	8.3 \pm 2.3	5.1 \pm 6.5	7.2 \pm 4.1	5.7 \pm 4.7	11.3	17.9
SO ₄ ²⁻	5.49 \pm 3.05	30.6 \pm 23.9	12.9 \pm 9.3	20.3 \pm 4.2	11.7 \pm 8.1	11.8 \pm 4.2	9.3 \pm 4.9	16.8	19.6
NH ₄ ⁺	3.87 \pm 2.59	12.3 \pm 10.8	6.6 \pm 6.2	9.9 \pm 2.1	5.6 \pm 5.3	6.7 \pm 3.4	4.2 \pm 4.2	9.7	9.2
Ca ²⁺	0.51 \pm 0.52	1.4 \pm 1.1	n.a.	3.4 \pm 2.4	1.2 \pm 0.7	2.2 \pm 0.9	n.a.	0.5	n.a.
K ⁺	0.62 \pm 0.65	3.6 \pm 5.6	0.9 \pm 0.9	1.8 \pm 0.9	1.1 \pm 0.9	1.2 \pm 0.5	n.a.	1.1	n.a.
F ⁻	0.05 \pm 0.02	0.4 \pm 0.3	n.a.	n.a.	2.1 \pm 3.6	0.5 \pm 0.2	n.a.	n.a.	n.a.
Cl ⁻	1.13 \pm 1.17	9.6 \pm 6.7	1.6 \pm 1.5	2.6 \pm 0.9	0.3 \pm 0.8	5.2 \pm 2.6	n.a.	1.2	n.a.
Na ⁺	0.38 \pm 0.22	1.8 \pm 1.0	n.a.	4.9 \pm 1.4	1.2 \pm 0.6	0.8 \pm 0.2	n.a.	0.2	n.a.
Mg ²⁺	0.14 \pm 0.12	0.4 \pm 0.6	n.a.	0.3 \pm 0.1	0.6 \pm 0.1	0.4 \pm 0.1	n.a.	0.1	n.a.
OC	10.5 \pm 5.49	37.5 \pm 23.9	7.0 \pm 8.4	n.a.	n.a.	35.4 \pm 13.9	14.9 \pm 7.5	n.a.	20.0
EC	1.45 \pm 0.97	14.7 \pm 12.3	1.0 \pm 0.8	n.a.	n.a.	13.8 \pm 5.4	2.8 \pm 1.2	n.a.	5.2

425 N: number; ^aData from Xu et al. (2016b); ^bData from Ming et al. (2017); ^cData from Dai et al. (2013); ^dData from Song et al. (2018); ^eData from
426 Tan et al. (2017); ^fData from Chen et al. (2016); ^gData from Huang et al. (2016); ^hData from Jiang et al. (2017).

427

428

429

430

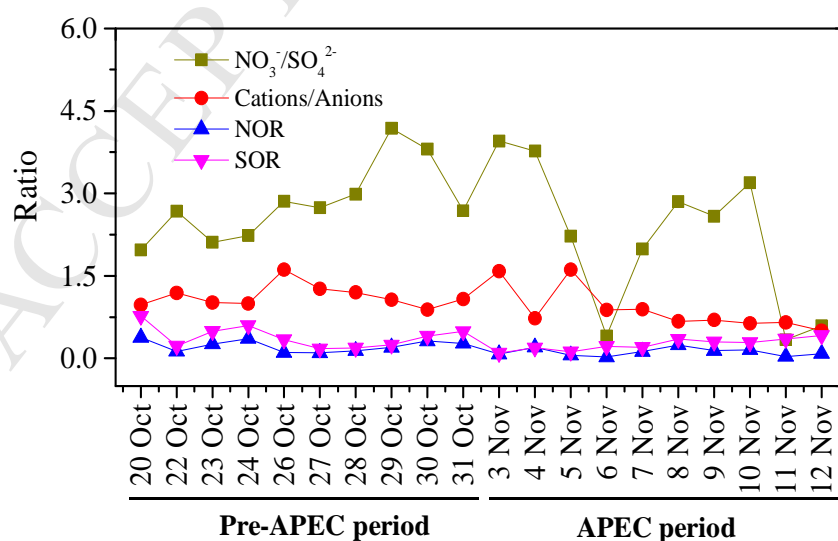
431 **Table 3.** Comparison of the concentrations of water-soluble inorganic ions in Beijing
 432 with other cities worldwide.

Location	Period	Concentration ($\mu\text{g m}^{-3}$)				
		NO_3^-	SO_4^{2-}	NH_4^+	OC	EC
Beijing, China ^a	3-12 Nov. 2014	13.4	5.5	3.9	10.5	1.5
Inchen, Korea ^b	Sep-Nov, 2009	3.5	4.9	3.3	7.9	2.0
Barcelona, Spain ^c	Feb-Dec, 2011	1.0	2.8	1.0	3.0	1.2
Marseille, France ^c	Jul 2011-Jul 2012	1.7	2.2	1.5	6.2	1.8
Genoa, Italy ^c	Mar-Sep, 2011	0.5	3.6	1.4	2.7	1.4
Venice, Italy ^c	Jan-Dec, 2011	5.4	3.4	2.3	n.a.	n.a.
Thessaloniki, Greece ^c	Jun 2011-May 2012	2.4	3.9	2.1	6.6	1.3
Košetic, Czech Republic ^d	Feb 2009-Apr 2010	2.2	2.9	1.5	4.1	0.6
Katowice, Poland ^e	Sep-Nov, 2010	2.5	4.2	2.0	3.3	2.5
Gdańsk, Poland ^e	Sep-Nov, 2010	1.9	1.9	0.8	2.2	1.7
Diabla Góra, Poland ^e	Sep-Nov, 2010	1.5	2.0	0.7	1.4	0.9
Cuernavaca, México ^f	May-Jun, 2012	0.4	3.6	1.7	n.a.	n.a.
Delhi, India ^g	Dec 2011-Nov 2012	8.9	19.1	5.8	33.5	6.9
Kathmandu Valley, Nepal ^h	Aug-Sep, 2014	0.1	3.7	2.3	n.a.	n.a.

433 ^aThis study; APEC period: 3-12 Nov. 2014; ^bData from Choi et al. (2012); ^cData from
 434 Salameh et al. (2015); ^dData from Schwarz et al. (2016); ^eData from Rogulakozłowska
 435 et al. (2014); ^fData from Saldarriaga-Noreña et al. (2014); ^gData from Dumka et al.
 436 (2017); ^hData from Shakya et al. (2017).

437
 438 The mass ratio of $\text{NO}_3^-/\text{SO}_4^{2-}$ can be used as an indicator of the relative
 439 importance of mobile versus stationary sources of nitrogen and sulfur in the
 440 atmosphere with high ratios indicating the predominance of mobile sources over
 441 stationary sources (Dai et al., 2018). In Beijing, the emission ratios of NO_x to SO_2
 442 from gasoline and diesel vehicles are 10:1 and 8:1, respectively, whereas those from
 443 coal combustion are less than 1.0 (Han et al., 2016). The average ratio of $\text{NO}_3^-/\text{SO}_4^{2-}$
 444 was 2.5 during the entire sampling period and was 23% lower in the APEC period (2.2)
 445 than in the pre-APEC period (2.8) (**Fig. 7**), indicating a dominant contribution from
 446 mobile vehicles rather than from coal-fueled industries. Factors influencing the
 447 $\text{NO}_3^-/\text{SO}_4^{2-}$ ratio include both the relative contributions of primary SO_2 and NO_x
 448 emissions as well as the chemical reactions determining formation of secondary
 449 inorganic aerosol.

450 To examine the degree of the secondary conversion from NO_2 to NO_3^- and from
 451 SO_2 to SO_4^{2-} , the nitrogen oxidation ratio ($\text{NOR} = n\text{NO}_3^- / (n\text{NO}_3^- + n\text{NO}_2)$) and the
 452 sulfur oxidation ratio ($\text{SOR} = n\text{SO}_4^{2-} / (n\text{SO}_4^{2-} + n\text{SO}_2)$) (n refers to the molar
 453 concentration) were calculated using daily concentrations of NO_3^- and SO_4^{2-} measured
 454 at the CAU site and the MEP-reported concentrations of NO_2 and SO_2 at the Wanliu
 455 monitoring station. The two sites are separated by only 7 km and therefore share
 456 similar pollution climates (Xu et al., 2017). The higher values of SOR and NOR
 457 indicate that more gaseous species would be oxidized to secondary aerosol in air. It
 458 has been reported that SOR was less than 0.10 in the primary source emissions and
 459 was greater than 0.10 when sulfate was produced through the photochemical
 460 oxidation of SO_2 (Wang et al., 2005). The average NOR and SOR during the entire
 461 measurement campaign were 0.17 and 0.32, respectively (**Fig. 7**), suggesting that
 462 higher secondary formation occurred for sulfate than for nitrate. Lower values of
 463 NOR and SOR were observed during the APEC period (0.12 and 0.16, respectively)
 464 compared with those in the pre-APEC period (0.23 and 0.39, respectively), which
 465 clearly indicates that the secondary transformation was relatively weaker in the APEC
 466 period. These results together with lower ratios of $\text{NO}_3^-/\text{SO}_4^{2-}$ in the APEC period also
 467 suggest the predominance of stationary pollutant sources over mobile sources,
 468 reflecting the impact of vehicle restrictions on the nitrate concentration. Overall,
 469 lower concentrations of SIA in the APEC period were attributed to a combination of
 470 reduced emissions and lower oxidation rates of SO_2 and NO_x .



471

472 **Fig. 7.** Daily average $\text{NO}_3^-/\text{SO}_4^{2-}$, cations/anions, sulfur oxidation ratio (SOR) and
 473 nitrogen oxidation ratio.

474

475 The gas-phase oxidation of SO_2 to sulfate by OH radical is a strong function of
476 temperature, whereas heterogeneous oxidation of SO_2 is positively correlated with
477 relative humidity (Sun et al., 2006). During the entire sampling period, relative
478 humidity was found to be positively correlated with NOR and SOR (both $p < 0.001$,
479 $r = 0.88$ and 0.59 , respectively). A significant positive correlation ($r = 0.47$, $p < 0.05$) was
480 found between NOR and temperature, whereas a moderate (but not significant)
481 positive correlation ($r = 0.41$, $p > 0.05$) was found between SOR and temperature (**Table**
482 **S1**). The results above suggested a major oxidation mechanism of NO_2 to NO_3^- , and
483 SO_2 to SO_4^{2-} is the aqueous phase oxidation of SO_2 instead of the gas-phase oxidation
484 (Jiang and Xia, 2017). In addition, both NOR and SOR showed strong positive and
485 highly significant (both $p < 0.001$) correlations with NH_4^+ (**Table S1**), indicating that
486 $(\text{NH}_4)_2\text{SO}_4$ and NH_4NO_3 are the main chemical forms of SO_4^{2-} and NO_3^- .

487 SO_4^{2-} , NO_3^- , and NH_4^+ primarily form from chemical reactions of NH_3 with acid
488 gases (e.g., H_2SO_4 and HNO_3) (Seinfeld and Pandis, 2006). NH_4^+ showed strong and
489 significant correlations with NO_3^- and SO_4^{2-} (both $p < 0.001$ and $r = 0.97$) (**Table 4**),
490 which is consistent with the results obtained from the analysis of correlations among
491 SOR, NOR, and NH_4^+ . Ammonia in aerosols in Beijing is preferentially neutralized by
492 H_2SO_4 to form $(\text{NH}_4)_2\text{SO}_4$ and/or NH_4HSO_4 , and the remaining components can react
493 with HNO_3 to form NH_4NO_3 (Sun et al., 2006). A strong and significant correlation
494 between SO_4^{2-} and NO_3^- was observed ($r = 0.94$, $p < 0.001$), suggesting that the fine
495 particulate NO_3^- was formed via heterogeneous reactions of HNO_3 and NH_3 on fully
496 neutralized fine particulate SO_4^{2-} , which is abundantly present in urban areas
497 (Ianniello et al., 2011).

498 Mg^{2+} mainly comes from mineral dust such as carbonate minerals (Wang et al.,
499 2005), as illustrated by the good correlation between Mg^{2+} and Ca^{2+} ($r = 0.68$, $p < 0.001$)
500 (**Table 4**). The measured concentrations of Mg^{2+} and Ca^{2+} throughout the sampling
501 period (0.19 ± 0.10 , and $0.93 \pm 0.60 \mu\text{g m}^{-3}$, respectively) were lower than those
502 reported in Xi'an, Shenzhen, Chengdu, and Lanzhou cities but were close to those
503 observed in Wuhan city (**Tables 1 and 2**). Significant reductions in the concentrations
504 of Mg^{2+} and Ca^{2+} (40% and 62%, respectively) in the APEC period (**Table 1**) reflect
505 an effective control on road and construction dust emissions. Traffic restriction
506 reduced turbulent re-suspension of road dust, resulting in a relatively lower Mg^{2+} and
507 Ca^{2+} concentrations.

508

509 **Table 4.** Correlation coefficients (Pearson's r) between the water-soluble inorganic
 510 ions, organic carbon (OC), and elemental carbon (EC).

	NO ₃ ⁻	SO ₄ ²⁻	NH ₄ ⁺	Ca ²⁺	K ⁺	F ⁻	Cl ⁻	Na ⁺	Mg ²⁺	OC	EC
NO ₃ ⁻	1.00										
SO ₄ ²⁻	0.94**	1.00									
NH ₄ ⁺	0.97**	0.97**	1.00								
Ca ²⁺	0.41	0.30	0.36	1.00							
K ⁺	0.86**	0.84**	0.86**	0.69**	1.00						
F ⁻	0.25	0.19	0.27	0.65**	0.42	1.00					
Cl ⁻	0.47*	0.34	0.38	0.65**	0.65**	0.17	1.00				
Na ⁺	0.80**	0.69**	0.78**	0.58**	0.84**	0.20	0.75**	1.00			
Mg ²⁺	0.43	0.34	0.42	0.68**	0.66**	0.29	0.64**	0.71**	1.00		
OC	0.87**	0.75**	0.80*	0.74**	0.92**	0.41	0.65**	0.83**	0.59*	1.00	
EC	0.56*	0.36	0.45	0.91**	0.82**	0.50*	0.78**	0.67**	0.62**	0.86**	1.00

511 * and ** denote significance at the 0.05 and 0.01 probability levels, respectively.

512

513 K⁺ is considered to be an acceptable indicator of biomass burning in Beijing
 514 (Wang et al., 2005). During our sampling period, we consider that biomass burning
 515 did not have a significant influence on K⁺ concentrations, given that the monitoring
 516 was conducted after the harvest of summer maize (mainly in October) in the vicinity
 517 of Beijing and thus open stalk burning had less influence. This notion is also reflected
 518 by fire maps (data available from
 519 <https://firms.modaps.eosdis.nasa.gov/download/create.php>) for Beijing and the
 520 surrounding regions; the number of fire points were comparable for the pre-APEC and
 521 APEC periods (327 versus 335) (**Fig. S3a, b**). The low average K⁺ concentrations
 522 ($0.62 \pm 0.65 \mu\text{g m}^{-3}$) during the APEC Blue period implied a minor contribution of
 523 biomass burning to PM_{2.5}. In addition, the 72-h air mass backward trajectories ending
 524 in Beijing (**Fig. S3c, d**) showed an absence of transport of air masses from the south
 525 of Beijing (in which heavy industry and intensive agriculture were located) in both the
 526 pre-APEC and APEC periods. Given this finding, the significant reductions in K⁺
 527 concentrations in the APEC period are most likely to be due to control of coal
 528 combustion because K⁺ in PM_{2.5} can originate from coal burning in the Jing-Jin-Ji
 529 megacities (Wang, 2013). In addition, the prevailing air masses during our sampling
 530 periods were from the northwest; thus, sea salt particles did not contribute
 531 significantly to measured ion concentrations (e.g., Na⁺, Cl⁻, Mg²⁺) (Xu et al., 2016a).

532 The Cl^- and Na^+ concentrations showed a significantly positive correlation ($r=0.75$,
533 $p<0.001$) (**Table 4**), suggesting a common origin of both ions. The mean Cl^-/Na^+
534 molar ratios were 1.55 and 1.78 in the pre-APEC and APEC periods, respectively, and
535 were higher than the mean ratio (1.17) of seawater (Zhang et al., 2013). These results
536 indicate the dominance of non-sea salt sources, of which the most likely contributor of
537 Cl^- is coal burning activities (Wang et al., 2005). This finding could subsequently
538 explain lower Cl^- concentrations in the APEC period due to reduced burning activities
539 for that time period. During combustion, vaporization of volatile elements, including
540 Na^+ , can occur from the surface of coal particles (Clarke, 1993). Furthermore, Cl^- was
541 significantly and positively correlated with K^+ , Ca^{2+} , and Mg^{2+} (**Table 4**), indicating
542 the presence of chloride salts such as, KCl , CaCl_2 , and MgCl_2 , other than NaCl at low
543 ambient temperature (Ianniello et al., 2011). In Beijing, KCl may also be released
544 from coal combustion, and CaCl_2 and MgCl_2 could be formed through heterogeneous
545 reactions of the dust carbonate with HCl emitted from coal combustion (Zhang et al.,
546 2013).

547 The ion balance is widely used as an indicator of the acidity of the aerosols using
548 the equivalent ratios of the total cations to the total anions in $\text{PM}_{2.5}$ (Zhang et al.,
549 2011). The cation and anion equivalents were calculated as follow:

$$550 \text{Cation equivalents} = \text{NH}_4^+/18 + \text{Ca}^{2+}/20 + \text{K}^+/39 + \text{Mg}^{2+}/12 + \text{Na}^+/23 \quad (4)$$

$$551 \text{Anion equivalents} = \text{Cl}^-/35.5 + \text{SO}_4^{2-}/48 + \text{NO}_3^-/62 + \text{F}^-/19 \quad (5)$$

552 The equivalent ratios of cations/anions (C/A) during the entire monitoring period
553 averaged 1.01 ± 0.33 (**Fig. 7**). The C/A ratio was higher than 1.0 during the pre-APEC
554 Blue period (1.13) but less than 1.0 during the APEC Blue period (0.89), indicating
555 the alkaline and acidic features of $\text{PM}_{2.5}$ samples, respectively. The higher C/A ratios
556 during the pre-APEC period may be the result of higher levels of carbonate and
557 bicarbonate (Clarke and Karani, 1992).

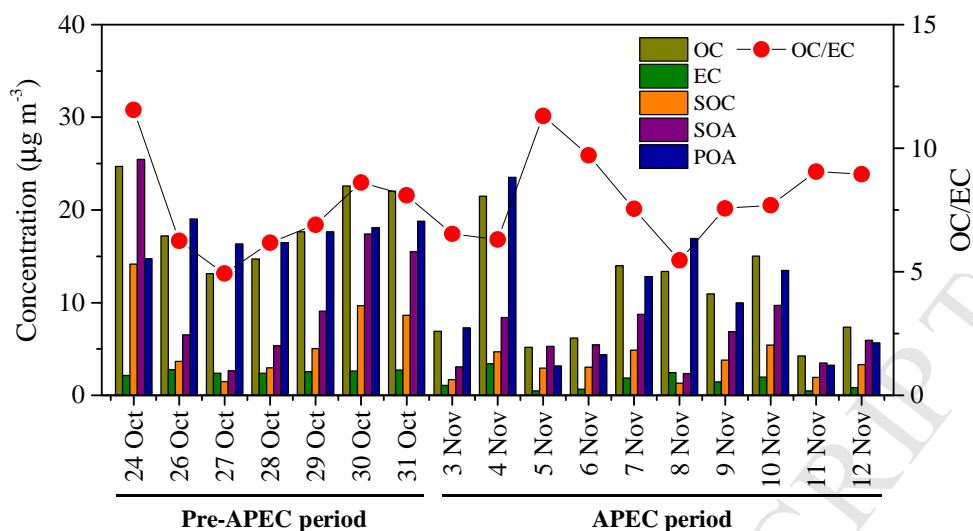
558 The mean concentrations of WSII in $\text{PM}_{2.5}$ in the Beijing atmosphere during the
559 summer and autumn seasons between 2008 and 2015 are shown in **Fig. S4**. The
560 concentrations of WSII in $\text{PM}_{2.5}$ during the APEC period were generally lower
561 compared with those measured in similar periods in 2009 and 2012-2013. This finding
562 could be ascribed to implementation of emission control measures. Although
563 comparable pollution control measures were enforced during the 2008 Olympics, the
564 2014 APEC Summit, and the 2015 Victory Day Parade, the WSII concentrations (e.g.,
565 NO_3^- , NH_4^+) were higher in the APEC period than the other two events, reflecting the

566 negative effects of unfavorable meteorological conditions as mentioned earlier (also
567 see Xu et al., 2016a). For instance, in autumn relatively low temperature in
568 combination with stable meteorological conditions (e.g. low wind speed and
569 atmospheric pressure) (Fig. 3) limit horizontal and vertical dispersion of atmospheric
570 pollutants, and further elevated levels of PM_{2.5} and chemical components.

571

572 3.3. Characteristics of carbonaceous aerosol

573 The concentrations of OC and EC during the sampling campaign averaged $13.9 \pm$
574 6.5 and $1.9 \pm 0.9 \mu\text{g m}^{-3}$, which are equal to 13 ± 5 and $2 \pm 1\%$ of the PM_{2.5} mass
575 concentration, respectively (**Fig. 8**). The results were comparable with those observed
576 during a similar sampling period at a rural site in Beijing (**Table 1**). In comparison
577 with other capital cities in China, the OC and EC concentrations during the APEC
578 period were lower than the values obtained in Xi'an, Lanzhou, Guangzhou and
579 Zhengzhou but higher than those observed in Shanghai (**Table 2**). In addition, the
580 concentration of OC in Beijing was higher than that observed in other regions globally
581 (with the exception of being approximately 3-fold lower than in India) (**Table 3**). In
582 contrast, the concentration of EC was comparable in Beijing to other cities worldwide
583 (except India). The average concentration of total carbon (TC, the sum of OC and EC)
584 during the APEC period significantly decreased by 79% compared with those in the
585 pre-APEC period with reductions of 45% and 43% for OC and EC, respectively
586 (**Table 1**). Previous studies reported that carbonaceous aerosols in Beijing primarily
587 originated from fossil fuel combustion from traffic, coal combustion in power plants
588 and industries (He et al., 2001) and from domestic heating and biomass burning
589 (Zhang et al., 2015b). Thus, the emission control measures taken during the APEC
590 Blue period, including prohibition of biomass burning, suspension of industrial
591 production, and reduction of the number of on-road vehicles, jointly contributed to
592 lower TC concentrations.



593

594 **Fig. 8.** Concentrations of carbonaceous compounds and OC/EC ratio in PM_{2.5}.

595

596 The OC and EC concentrations were found to be positively and significantly
 597 correlated ($r=0.86$, $p<0.001$) throughout the sampling period (**Table 4**), indicating
 598 some common origins, such as traffic emission and coal combustion. The OC/EC ratio
 599 is widely used to diagnose sources of carbonaceous aerosols and for estimation of
 600 SOC (Zhao et al., 2013). For example, the OC/EC ratio from biomass burning is
 601 particularly high within the range of 2.6-5.7 (Schmidl et al., 2008); however,
 602 fossil-fuel emissions tend to have low OC/EC ratios that are generally less than 1.0
 603 (Handler et al., 2008). As shown in **Fig. 8**, the OC/EC mass ratios fell within the range
 604 of 5-12, with means of 7.5 and 8.0 in the pre-APEC and APEC periods, respectively.
 605 Given the minimal influence of biomass burning (mentioned in Section 3.2), an
 606 explanation for higher OC/EC values in this study is that a stable atmosphere and low
 607 temperatures (Fig. 3) can facilitate the accumulation of air pollutants and create
 608 conditions for the condensation or adsorption of volatile organic compounds and thus
 609 elevated OC levels.

610 An OC/EC ratio of greater than 2.0 indicates the presence of SOC (Choi et al.,
 611 2012). Based on the EC-tracer method and the minimum OC/EC ratio of 4.93
 612 observed in this study, the estimated SOC concentration was $4.6 \pm 3.4 \mu\text{g m}^{-3}$
 613 ($1.3\text{-}14.2 \mu\text{g m}^{-3}$) (**Fig. 8**), accounting for 33% of OC and 4% of PM_{2.5} mass
 614 concentration, respectively. This finding indicates that SOC contributed a significant
 615 fraction of OC in PM_{2.5} during the entire sampling period. A nonsignificant reduction
 616 (on average 49%) in the SOC concentration was observed in the APEC Blue period

617 $(6.5 \pm 4.5 \mu\text{g m}^{-3})$ compared with the pre-APEC period $(3.3 \pm 1.4 \mu\text{g m}^{-3})$. Our
618 estimated SOC concentration $(4.6 \mu\text{g m}^{-3})$ was close to the mean value of $4.9 \mu\text{g m}^{-3}$
619 observed during the APEC period in rural Beijing (Wang et al., 2017). However, the
620 number of samples in this study is relatively limited, and the minimum of OC/EC was
621 likely not the real OC/EC of primary emissions. For example, Dan et al. (2004)
622 measured the OC/EC ratios in $\text{PM}_{2.5}$ and calculated a minimum OC/EC ratio of 0.9 for
623 the 2001-2003 period in Beijing. A similar minimum OC/EC ratio of 1.5 was
624 observed in PM_{10} during autumn in Beijing (Duan et al., 2005). Given that it is not
625 easy to determine the primary OC/EC ratios comprehensively because they are source
626 dependent and influenced by meteorological conditions, a more accurate estimate of
627 SOC during the APEC period is recommended in further work.

628 The average POA concentrations were significantly reduced by 42% during the
629 APEC period compared with the pre-APEC period $(10.0 \pm 6.7$ versus $17.3 \pm 1.5 \mu\text{g}$
630 $\text{m}^{-3})$, whereas a nonsignificant reduction of 49% was found for the average SOA
631 concentration between these two periods $(5.9 \pm 2.5$ versus 11.7 ± 8.1 (**Fig. 8**). The
632 SOC and SOA in air are affected by meteorological conditions with higher
633 temperature promoting their formation. The formation of SOC is limited when the
634 temperature is below 15°C (Strader et al., 1999). The average temperature was $13.6 \pm$
635 1.8°C during the pre-APEC period and $9.7 \pm 2.5^\circ\text{C}$ during the APEC period (**Fig. 3**).
636 Thus, the photochemical reactions resulting in secondary pollution were not active;
637 SOC and SOA reductions were mainly due to reduced gas-to-particle conversion
638 resulting from decreased emissions of semi-volatile and volatile organic compounds.
639 Similarly, the reduction of POA can be ascribed to primary emission control as POA is
640 emitted primarily from combustion processes (Wang et al., 2017).

641
642
643
644
645
646
647
648
649
650

651 **4. Conclusions**

652 We systematically quantified the impacts of stringent pollution control measures
653 on PM_{2.5} and its chemical components together with NH₃, NO₂ and other major air
654 pollutants before and during the APEC period in Beijing. Overall, the average
655 concentrations of water-soluble ions and carbonaceous species of PM_{2.5} showed
656 statistically significant reductions (29-78%) during the APEC period compared with
657 the pre-APEC period. SIA (34%) and OC (13%) were the main contributors to PM_{2.5}.
658 Lower concentrations of SIA in the APEC period were ascribed to effective emission
659 control and lower oxidation rates of SO₂ and NO_x. PM_{2.5} was alkaline in the
660 pre-APEC period but acidic in the APEC period. An OC/EC ratio exceeding 2.0
661 indicated that SOA was present during the entire sampling campaign.

662 Average NH₃ concentrations across all road sites significantly decreased in the
663 APEC period due to vehicle restrictions. Additionally, the satellite NH₃ columns over
664 Beijing demonstrated lower NH₃ concentration in the same period. Reducing traffic
665 NH₃ emissions could therefore be an effective approach to mitigate atmospheric NH₃
666 and secondary NH₄⁺ salt in PM_{2.5} in Beijing.

667 Emission control measures taken in the APEC period significantly decreased
668 PM_{2.5} pollution and other major pollutant (PM₁₀, NO₂, SO₂, and CO) concentrations at
669 a city level but significantly increased ground O₃ concentrations. Future emission
670 control measures should balance the trade-off between PM_{2.5} and O₃ pollution.

671

672 **Acknowledgements**

673 This work was supported by China National Funds for Distinguished Young Scientists
674 (41425007), the National Key R&D Program of China (2017YFC0210101,
675 2017YFC0210106), China Postdoctoral Science Foundation (2018M641531), the
676 National Natural Science Foundation of China (41705130), the National Ten-thousand
677 Talents Program of China (Xuejun Liu) as well as the SUNRISE programme funded
678 by the Natural Environment Research Council (NERC) as part of a National
679 Capability Long-Term Science - Official Development Assistance Award.

680

681 **Competing interests**

682 The authors declare that they have no conflict of interest.

683

684

685

686

687

688 **References**

689 Beijing Municipal Environmental Protection Bureau (BMEPB), 2014, viewed May 5,
690 2017, <http://www.bjepb.gov.cn/bjepb/332423/332446/416697/index.html>.

691 Chang, Y.H., Liu, X.J., Deng, C.R., Dore, A.J., Zhuang, G.S., 2016. Source
692 apportionment of atmospheric ammonia before, during, and after the 2014 APEC
693 summit in Beijing using stable nitrogen isotope signatures. *Atmos. Chem. Phys.* 16,
694 11635-11647.

695 Chen, C., Sun, Y.L., Xu, W.Q., Du, W., Zhou, L.B., Han, T.T., Wang, Q.Q., Fu, P.Q.,
696 Wang, Z.F., Gao, Z.Q., Zhang, Q., Worsnop, D.R., 2015. Characteristics and
697 sources of submicron aerosols above the urban canopy (260 m) in Beijing, China,
698 during the 2014 APEC summit. *Atmos. Chem. Phys.* 15, 12879-12895.

699 Chen, W.H., Wang, X.M., Zhou, S.Z., Cohen, J.B., Zhang, J.P., Wang, Y., Chang, M.,
700 Zeng, Y.J., Liu, Y.X., Lin, Z.H., 2016. Chemical Composition of PM_{2.5} and its
701 Impact on Visibility in Guangzhou, Southern China. *Aerosol Air Qual. Res.* 16,
702 2349-2361.

703 Choi, J.K., Heo, J.B., Ban, S.J., Yi, S.M., Zoh, K.D., 2012. Chemical characteristics
704 of PM_{2.5} aerosol in Incheon, Korea. *Atmos. Environ.* 60, 583-592.

705 Chow, J.C., Watson, J.G., Chen, L.W.A., Oliver Chang, M.C., Robinson, N.F.,
706 Trimble, D., Kohl, S., 2007. The IMPROVE_A temperature protocol for
707 thermal/optical carbon analysis: maintaining consistency with a long-term database.
708 *Atmos. Environ. A Gen. Top.* 27, 1185-1201.

709 Clarke, A.G., Karani, G.N., 1992. Characterisation of the carbonate content of
710 atmospheric aerosols. *J. Atmos. Chem.* 14, 119-128.

711 Clarke, L.B., 1993. The fate of trace elements during coal combustion and gasification:
712 an overview. *Fuel* 72, 731-736.

713 Cohen, A.J., Brauer, M., Burnett, R., Anderson, H.R., Frostad, J., Estep, K.,
714 Balakrishnan, K., Brunekreef, B., Dandona, L., Dandona, R., Feigin, V., Freedman,
715 G., Hubbell, B., Jobling, A., Kan, H., Knibbs, L., Liu, Y., Martin, R., Morawska, L.,
716 Pope Iii, C.A., Shin, H., Straif, K., Shaddick, G., Thomas, M., van Dingenen, R.,
717 van Donkelaar, A., Vos, T., Murray, C.J.L., Forouzanfar, M.H., 2017. Estimates and
718 25-year trends of the global burden of disease attributable to ambient air pollution:
719 an analysis of data from the Global Burden of Diseases Study 2015. *Lancet* 389,

- 720 1907-1918.
- 721 Dai, Q.L., Bi, X.H., Liu, B.S., Li, L.W., Ding, J., Song, W.B., Bi, S.Y., Schulze, B.C.,
722 Song, C.B., Wu, J.H., Zhang, Y.F., Feng, Y.C., Hopke, P.K., 2018. Chemical
723 nature of PM_{2.5} and PM₁₀ in Xi'an, China: Insights into primary emissions and
724 secondary particle formation. *Environ. Pollut.* 240, 155-166.
- 725 Dai, W., Gao, J.Q., Cao, G., Ouyang, F., 2013. Chemical composition and source
726 identification of PM_{2.5} in the suburb of Shenzhen, China. *Atmos. Res.* 122,
727 391-400.
- 728 Dan, M., Zhuang, G., Li, X., Tao, H., Zhuang, Y., 2004. The characteristics of
729 carbonaceous species and their sources in PM_{2.5} in Beijing. *Atmos. Environ.* 38,
730 3443-3452.
- 731 Ding, A.J., Huang, X., Nie, W., Sun, J.N., Kerminen, V.M., Petäjä, T., Su, H., Cheng,
732 Y.F., Yang, X.Q., Wang, M.H., Chi, X.G., Wang, J.P., Virkkula, A., Guo, W.D.,
733 Yuan, J., Wang, S.Y., Zhang, R.J., Wu, Y.F., Song, Y., Zhu, T., Zilitinkevich, S.,
734 Kulmala, M., Fu, C.B., 2016. Enhanced haze pollution by black carbon in
735 megacities in China. *Geophys. Res. Lett.* 43, 2873-2879.
- 736 Draxler, R., Stunder, B., Rolph, G., Stein, A., Taylor, A., 2012. HYSPLIT4 user's
737 guide, version 4, report, NOAA, Silver Spring, MD.
- 738 Duan, F., He, K., Ma, Y., Jia, Y., Yang, F., Lei, Y., Tanaka, S., Okuta, T., 2005.
739 Characteristics of carbonaceous aerosols in Beijing, China. *Chemosphere* 60,
740 355-364.
- 741 Dumka, U.C., Tiwari, S., Kaskaoutis, D.G., Hopke, P.K., Singh, J., Srivastava, A.K.,
742 Bisht, D.S., Attri, S.D., Tyagi, S., Misra, A., Pasha, G.S.M., 2017. Assessment of
743 PM_{2.5} chemical compositions in Delhi: primary vs secondary emissions and
744 contribution to light extinction coefficient and visibility degradation. *J. Atmos.*
745 *Chem.* 74, 423-450.
- 746 Gao, M., Liu, Z.R., Wang, Y.S., Lu, X., Ji, D.S., Wang, L.L., Li, M., Wang, Z.F.,
747 Zhang, Q., Carmichael, G.R., 2017. Distinguishing the roles of meteorology,
748 emission control measures, regional transport, and co-benefits of reduced aerosol
749 feedbacks in "APEC Blue". *Atmos. Environ.* 167, 476-486.
- 750 Gu, Y., Yim, S.H.L., 2016. The air quality and health impacts of domestic
751 trans-boundary pollution in various regions of China. *Environ. Int.* 97, 117-124.
- 752 Guo, J.P., Deng, M.J., Lee, S.S., Wang, F., Li, Z.Q., Zhai, P.M., Liu, H., Lv, W.T.,
753 Yao, W., Li, X.W., 2016. Delaying precipitation and lightning by air pollution over

- 754 the Pearl River Delta. Part I: Observational analyses. *J. Geophys. Res. Atmos.* 121,
755 6472-6488.
- 756 Guo, J.P., Su, T.N, Li, Z.Q, Miao, Y.C, Li, J., Liu, H., Xu, H., Cribb, M., Zhai, P.M.,
757 2017. Declining frequency of summertime local-scale precipitation over eastern
758 China from 1970-2010 and its potential link to aerosols. *Geophys. Res. Lett.* 44,
759 5700-5708.
- 760 Han, X.K., Guo, Q.J., Liu, C.Q., Strauss, H., Yang, J.X., Hu, J., Wei, R.F., Tian, L.Y.,
761 Kong, J., Peters, M., 2016. Effect of the pollution control measures on PM_{2.5} during
762 the 2015 China Victory Day Parade: Implication from water-soluble ions and sulfur
763 isotope. *Environ. Pollut.* 218, 230-241.
- 764 Handler, M., Puls, C., Zbiral, J., Marr, I., Puxbaum, H., Limbeck, A., 2008. Size and
765 composition of particulate emissions from motor vehicles in the
766 KaisermühlenTunnel, Vienna. *Atmos. Environ.* 42, 2173-2186.
- 767 He, K.B., Yang, F.M., Ma, Y.L., Zhang, Q., Yao, X.H., Chan, C.K., Cadle, S., Chan,
768 T., Mulawa, P., 2001. The characteristics of PM_{2.5} in Beijing, China. *Atmos.*
769 *Environ.* 35, 4959-4970.
- 770 Hua, Y., Cheng, Z., Wang, S., Jiang, J., Chen, D., Cai, S., Fu, X., Fu, Q., Chen, C.,
771 Xu, B., Yu, J., 2015. Characteristics and source apportionment of PM_{2.5} during a
772 fall heavy haze episode in the Yangtze River Delta of China. *Atmos. Environ.* 123
773 (Part B), 380-391.
- 774 Huang, T., Chen, J., Zhao, W.T., Cheng, J.X., Cheng, S.G., 2016. Seasonal variations
775 and correlation analysis of water-soluble inorganic ions in PM_{2.5} in Wuhan, 2013.
776 *Atmosphere* 7, 49.
- 777 Huang, R.J., Zhang, Y., Bozzetti, C., Ho, K.F., Cao, J.J., Han, Y., Daellenbach, K.R.,
778 Slowik, J.G., Platt, S.M., Canonaco, F., Zotter, P., Wolf, R., Pieber, S.M., Bruns,
779 E.A., Crippa, M., Ciarelli, G., Piazzalunga, A., Schwikowski, M., Abbaszade, G.,
780 SchnelleKreis, J., Zimmermann, R., An, Z., Szidat, S., Baltensperger, U., Haddad,
781 I.E., Prevot, A.S.H., 2014. High secondary aerosol contribution to particulate
782 pollution during haze events in China. *Nature* 514, 218-222.
- 783 Ianniello, A., Spataro, F., Esposito, G., Allegrini, I., Rantica, E., Ancora, M. P., Hu,
784 M., Zhu, T., 2010. Occurrence of gas phase ammonia in the area of Beijing (China).
785 *Atmos. Chem. Phys.* 10, 9487-9503.
- 786 Ianniello, A., Spataro, F., Esposito, G., Allegrini, I., Hu, M., Zhu, T., 2011. Chemical
787 characteristics of inorganic ammonium salts in PM_{2.5} in the atmosphere of Beijing

- 788 (China). *Atmos. Chem. Phys.* 11, 10803-10822.
- 789 Jiang, B.F., Xia, D.H., 2017. Role identification of NH_3 in atmospheric secondary
790 new particle formation in haze occurrence of China. *Atmos. Environ.* 163, 107-117.
- 791 Jiang, J.K., Zhou, W., Cheng, Z., Wang, S.X., He, K.B., Hao, J.M., 2017. Particulate
792 matter distribution in China during a winter period with frequent pollution episodes
793 (January 2013). *Aerosol Air Qual. Res.* 15, 494-503.
- 794 Kaufman, Y.J., Tanré, D., Boucher, O., 2002. A satellite view of aerosols in the
795 climate system. *Nature* 419, 215-223.
- 796 Koren, I., Dagan, G., Altaratz, O., 2014. From aerosol-limited to invigoration of warm
797 convective clouds. *Science*. 344, 1143-1146.
- 798 Li J, Chen, H.B., Li, Z.Q., Wang, P.C., Cribb, M., Fan, X.H., 2015. Low-level
799 temperature inversions and their effect on aerosol condensation nuclei
800 concentrations under different large-scale synoptic circulations. *Adv. Atmos. Sci.*
801 32, 898-908.
- 802 Li, K., Jacob, D.J., Liao, H., Shen, L., Zhang, Q., Bates, K.H., 2019. Anthropogenic
803 drivers of 2013–2017 trends in summer surface ozone in China. *Proc Natl Acad Sci*
804 *USA*. 116, 422-427.
- 805 Li, Z.Q., Guo, J.P., Ding, A.J., Liao, H., Liu, J.J., Sun, Y.L., Wang, T.J., Xue, H.W.,
806 Zhang, H.S., Zhu, B., 2017. Aerosol and boundary-layer interactions and impact on
807 air quality. *Natl. Sci. Rev.* 4, 810-833.
- 808 Liu, X.J., Xu, W., Duan, L., Du, E.Z., Pan, Y.P., Lu, X.K., Zhang, L., Wu, Z.Y.,
809 Wang, X.M., Zhang, Y., Shen, J.L., Song, L., Feng, Z.Z., Liu, X.Y., Song, W.,
810 Tang, A.H., Zhang, Y.Y., Zhang, X.Y., Collett, Jr. J.L., Chang, Y.H., 2017a.
811 Atmospheric nitrogen emission, deposition and air quality impacts in China: An
812 overview. *Curr. Pollut. Rep.* 3, 65-77.
- 813 Liu, H.L., He, J., Guo, J.P., Miao, Y.C., Yin, J.F., Wang, Y., Xu, H., Liu, H., Yan, Y.,
814 Li, Y., Zhai, P.M., 2017b. The blue skies in Beijing during APEC 2014: A
815 quantitative assessment of emission control efficiency and meteorological influence.
816 *Atmos. Environ.* 167, 235-244.
- 817 Liu, L., Zhang, X., Xu, W., Liu, X., Li, Y., Lu, X., Zhang, Y., Zhang, W., 2017c.
818 Temporal characteristics of atmospheric ammonia and nitrogen dioxide over China
819 based on emission data, satellite observations and atmospheric transport modeling
820 since 1980. *Atmos. Chem. Phys.* 17, 9365-9378.
- 821 Ma, J.Z., Chu, B.W., Liu, J., Liu, Y.C., Zhang, H.X., He, H., 2018. NO_x promotion of

- 822 SO₂ conversion to sulfate: An important mechanism for the occurrence of heavy
823 haze during winter in Beijing. *Environ. Pollut.* 233, 662-669.
- 824 Ming, L.L., Jin, L., Li, J., Fu, P., Yang, W., Liu, D., Zhang, G., Wang, Z., Li, X.,
825 2017. PM_{2.5} in the Yangtze River Delta, China: Chemical compositions, seasonal
826 variations, and regional pollution events. *Environ. Pollut.* 223, 200-212.
- 827 Pant, P., Shukla, A., Kohl, S.D., Chow, J.C., Watson, J.G., Harrison, P.M., 2015.
828 Characterization of ambient PM_{2.5} at a pollution hotspot in New Delhi, India and
829 inference of sources. *Atmos. Environ.* 109, 178-189.
- 830 Paschalidou, A.K., Kassomenos, P.A., 2004. Comparison of air pollutant
831 concentrations between weekdays and weekends in Athens, Greece for various
832 meteorological conditions. *Environ. Technol.* 25, 1241-1255.
- 833 Petäjä, T., Järvi, L., Kerminen, V.-M., Ding, A.J., Sun, J.N., Nie, W., Kujansuu, J.,
834 Virkkula, A., Yang, X., Fu, C.B., Zilitinkevich, S., Kulmala, M., 2016. Enhanced
835 air pollution via aerosolboundary layer feedback in China. *Sci Rep.* 6, 18998.
- 836 Philip, S., Martin, R.V., Pierce, J.R., Jimenez, J.L., Zhang, Q., Canagaratna, M.R.,
837 Spracklen, D.V., Nowlan, C.R., Lamsal, L.N., Cooper, M.J., Krotkov, N.A., 2014.
838 Spatially and seasonally resolved estimate of the ratio of organic mass to organic
839 carbon. *Atmos. Environ.* 87, 34-40.
- 840 Pöschl, U., 2005. Atmospheric aerosols: composition, transformation, climate and
841 health effects. *Angew. Chem. Int. Edit.* 44, 7520-7540.
- 842 Puchalski, M.A., Sather, M.E., Walker, J.T., Lelunann, C.M.B., Gay, D.A., Mathew,
843 J., Robargef, W.P., 2011. Passive ammonia monitoring in the United States:
844 Comparing three different sampling devices. *J. Environ. Monitor.* 13, 3156-3167.
- 845 Rogulakozłowska, W., Klejnowski, K., Rogulakopiec, P., Ośródk, L., Krajny, E.,
846 Błaszczak, B., Mathews, B., 2014. Spatial and seasonal variability of the mass
847 concentration and chemical composition of PM_{2.5} in Poland. *Air Qual. Atmos. Hlth.*
848 7, 41-58.
- 849 Salameh, D., Detournay, A., Pey, J., Perez, N., Liguori, F., Saraga, D., Chiara Bove,
850 M., Brotto, P., Cassola, F., Massabo, D., Latella, A., Pillon, S., Formenton, G., Patti,
851 S., Armengaud, A., Piga, D., Jaffrezo, J.L., Bartzis, J., Tolis, E., Prati, P., Querol,
852 X., Wortham, H., Marchand, N., 2015. PM_{2.5} chemical composition on five
853 European Mediterranean cities: a 1-year study. *Atmos. Res.* 155, 102-177.
- 854 Saldarriaga-Noreña, H., Hernández-Mena, L., Sánchez-Salinas, E., Ramos-Quintana,
855 F., Ortíz-Hernández, L., Morales-Cueto, R., Alarcón-González, V.,

- 856 Ramírez-Jiménez, S., 2014. Ionic composition in aqueous extracts from PM_{2.5} in
857 ambient air at the city of Cuernavaca, México. *J. Environ. Prod.* 5, 1305-1315.
- 858 Schwarz, J., Cusack, M., Karban, J., Chalupníčková, E., Havránek, V., Smolík, J.,
859 Ždímal, V., 2016. PM_{2.5} chemical composition at a rural background site in Central
860 Europe, including correlation and air mass back trajectory analysis. *Atmos. Res.*
861 176-177, 108-120.
- 862 Schleicher, N., Norra, S., Chen, Y., 2012. Efficiency of mitigation measures to reduce
863 particulate air pollution-a case study during the Olympic Summer Games 2008 in
864 Beijing, China. *Sci. Total Environ.* 427-428, 146-158.
- 865 Schmidl, C., Marr, I.L., Caseiro, A., Kotianov a, P., Berner, A., Bauer, H.,
866 Kasper-Giebl, A., Puxbaum, H., 2008. Chemical characterisation of fine particle
867 emissions from wood stove combustion of common woods growing in
868 mid-European Alpine regions. *Atmos. Environ.* 42, 126-141.
- 869 Seinfeld, J. H., Pandis, S. N., 2006. *Atmospheric chemistry and physics: from air
870 pollution to climate change*, 2nd Edn., Wiley Interscience, New Jersey.
- 871 Shakya, K.M., Peltier, R.E., Shrestha, H., Byanju, R.M., 2017. Measurements of TSP,
872 PM₁₀, PM_{2.5}, BC, and PM chemical composition from an urban residential location
873 in Nepal. *Atmos. Pollut. Res.* 8, 1123-1131.
- 874 Shen, J.L., Tang, A.H., Liu, X.J., Kopsch, J., Fangmeier, A., Goulding, K., Zhang,
875 F.S., 2011. Impacts of pollution controls on air Quality in Beijing during the 2008
876 Olympic Games. *J. Environ. Qual.* 40, 37-45.
- 877 Song, L., Liu, X.J., Skiba, U., Zhu, B., Zhang, X.F., Liu, M.Y., Twigg, M., Shen, J.L.,
878 Dore, A., Reis, S., Coyle, M., Zhang, W., Levy, P., Fowler, D., 2018. Ambient
879 concentrations and deposition rates of selected reactive nitrogen species and their
880 contribution to PM_{2.5} aerosols at three locations with contrasting land use in
881 southwest China. *Environ. Pollut.* 233, 1164-1176.
- 882 Strader, R., Lurmann, F., Pandis, S.N., 1999. Evaluation of secondary organic aerosol
883 formation in winter. *Atmos. Environ.* 33, 4849-4863.
- 884 Sun, Y.L., Zhuang, G.S., Tang, A.H., Wang, Y., An, Z. H., 2006. Chemical
885 Characteristics of PM_{2.5} and PM₁₀ in haze-fog episodes in Beijing. *Environ. Sci.*
886 *Technol.* 40, 3148-3155.
- 887 Sun, Y.L., Jiang, Q., Wang, Z.F., Fu, P.Q., Li, J., Yang, T., Yin, Y., 2014.
888 Investigation of the sources and evolution processes of severe haze pollution in
889 Beijing in January 2013. *J. Geophys. Res.* 119, 4380-4398.

- 890 Sun, Y.L., Wang, Z.F., Wild, O., Xu, W.Q., Chen, C., Fu, P.Q., Du, W., Zhou, L.B.,
891 Zhang, Q., Han, T.T., Wang, Q.Q., Pan, X.L., Zheng, H.T., Li, J., Guo, X.F., Liu,
892 J.G., Worsnop, D.R., 2016. "APEC Blue": Secondary Aerosol Reductions from
893 Emission Controls in Beijing. *Sci. Rep.* 6, 20668.
- 894 Tan, J.H., Zhang, L.M., Zhou, X.M., Duan, J.C., Li, Y., Hu, J.N., He, K.B., 2017.
895 Chemical characteristics and source apportionment of PM_{2.5} in Lanzhou, China. *Sci.*
896 *Total Environ.* 601-602, 1743-1752.
- 897 Tao, Y., Yin, Z., Ye, X.N., Ma, Z., Chen, J.M., 2014. Size distribution of
898 water-soluble inorganic ions in urban aerosols in Shanghai. *Atmos. Pollut. Res.* 5,
899 639-647.
- 900 Tang, Y.S., Cape, J.N., Sutton, M.A., 2001. Development and types of passive
901 samplers for monitoring atmospheric NO₂ and NH₃ concentrations. *The Scientific*
902 *World J.* 1, 513-529.
- 903 Van Damme, M., Whitburn, S., Clarisse, L., Clerbaux, C., Hurtmans, D., Coheur, P.F.,
904 2017. Version 2 of the IASI NH₃ neural network retrieval algorithm: near-real-time
905 and reanalysed datasets. *Atmos. Meas. Tech.* 10, 1-14.
- 906 Wang, G., Cheng, S., Wei, W., Yang, X., Wang, X., Jia, J., Lang, J., Lv, Z., 2017.
907 Characteristics and emission-reduction measures evaluation of PM_{2.5} during the two
908 major events: APEC and Parade. *Sci. Total Environ.* 595, 81-92.
- 909 Wang, H.B., Tian, M., Chen, Y., Shi, G.M., Liu, Y., Yang, F.M., Zhang, L.M., Deng,
910 L.Q., Yu, J.Y., Peng, C., Cao, X.Y., 2018. Seasonal characteristics, formation
911 mechanisms and source origins of PM_{2.5} in two megacities in Sichuan Basin, China.
912 *Atmos. Chem. Phys.* 18, 865-881.
- 913 Wang, L., 2013. Characteristics of Water-soluble Inorganic Ions in Aerosol Particles
914 in JingJinJi-mega Typical Cities (Master thesis). Beijing University of Chemical
915 Technology, Beijing, China (in Chinese).
- 916 Wang, Y., Zhuang, G.S., Tang, A.H., Yuan, H., Sun, Y.L., Chen, S., Zheng, A.H.,
917 2005. The ion chemistry and the source of PM_{2.5} aerosol in Beijing. *Atmos.*
918 *Environ.* 39, 3771-3784.
- 919 Wang, Y., Zhang, Y., Schauer, J.J., Foy, B.D., Guo, B., Zhang, Y.X., 2016. Relative
920 impact of emissions controls and meteorology on air pollution mitigation associated
921 with the Asia-Pacific Economic Cooperation (APEC) conference in Beijing, China.
922 *Sci. Total Environ.* 571, 1467-1476.
- 923 Xu, J., Zhang, Q., Chen, M., Ge, X., Ren, J., Qin, D., 2014. Chemical composition,

- 924 sources, and processes of urban aerosols during summertime in northwest china:
925 Insights from high resolution aerosol mass spectrometry. *Atmos. Chem. Phys.* 14,
926 12593-12611.
- 927 Xu, W., Wu, Q.H., Liu, X.J., Tang, A.H., Dore, A.J., Heal, M.R., 2016a.
928 Characteristics of ammonia, acid gases, and PM_{2.5} for three typical land-use types in
929 the North China Plain. *Environ. Sci. Pollut. Res.* 23, 1158-1172.
- 930 Xu, H.M., Cao, J.J., Chow, J.C., Huang, R. J., Shen, Z.X., Chen, L. W. A., Ho, K.F.,
931 Watson, J.G., 2016b. Inter-annual variability of wintertime PM_{2.5} chemical
932 composition in Xi'an, China: Evidences of changing source emissions. *Sci. Total*
933 *Environ.* 545-546, 546-555.
- 934 Xu, J.Z., Zhang, Q., Wang, Z.B., Yu, G.M., Ge, X.L., Qin, X., 2015. Chemical
935 composition and size distribution of summertime PM_{2.5} at a high altitude remote
936 location in the northeast of the Qinghai-Xizang (Tibet) Plateau: insights into
937 aerosol sources and processing in free troposphere. *Atmos. Chem. Phys.* 15,
938 5069-5081.
- 939 Xu, W., Song, W., Zhang, Y., Liu, X., Zhang, L., Zhao, Y., Liu, D., Tang, A., Yang,
940 D., Wang, D., Wen, Z., Pan, Y., Fowler, D., Collett Jr., J.L., Erisman, J.W.,
941 Goulding, K., Li, Y., Zhang, F., 2017. Air quality improvement in a megacity:
942 implications from 2015 Beijing Parade Blue pollution control actions. *Atmos.*
943 *Chem. Phys.* 17, 31-46.
- 944 Yu, H.B, Liu, S.C., Dickinson, R.E., 2002. Radiative effects of aerosols on the
945 evolution of the atmospheric boundary layer. *J. Geophys. Res.* 107, 4142.
- 946 Yue, X., Unger, N., Harper, K., Xia, X.G., Liao, H., Zhu, T., Xiao, J.F., Feng, Z.Z., Li,
947 J., 2017. Ozone and haze pollution weakens net primary productivity in China.
948 *Atmos. Chem. Phys.* 17, 6073-6089.
- 949 Zhao, P.S, Dong, F., Yang, Y.D., He, D., Zhao, X.J., Zhang, W.Z., Yao, Q., Liu, H.Y.,
950 2013. Characteristics of carbonaceous aerosol in the region of Beijing, Tianjin, and
951 Hebei, China. *Atmos. Environ.* 71, 389-398.
- 952 Zhang, H.F., Wang, S.X., Hao, J.M., Wang, X.M., Wang, S.L., Chai, F.H., Li, M.,
953 2016a. Air pollution and control action in Beijing. *J. Clean Prod.* 112, 1519-1527.
- 954 Zhang, Y., Huang, W., Cai, T., Fang, D., Wang, Y., Song, J., Hu, M., Zhang, Y.,
955 2016b. Concentrations and chemical compositions of fine particles (PM_{2.5}) during
956 haze and non-haze days in Beijing. *Atmos. Res.* 174, 62-69.
- 957 Zhang, J.K., Sun, Y., Liu, Z.R., Ji, D.S., Hu, B., Liu, Q., Wang, Y.S., 2014.

- 958 Characterization of submicron aerosols during a month of serious pollution in
959 Beijing, 2013. *Atmos. Chem. Phys.* 14, 2887-2903.
- 960 Zhang, T., Cao, J.J., Tie, X. X., Shen, Z.X., Liu, S.X., Ding, H., Han, Y.M., Wang, G.
961 H., Ho, K.F., Qiang, J., Li, W. T., 2011. Water-soluble ions in atmospheric aerosols
962 measured in Xi'an, China: Seasonal variations and sources. *Atmos. Res.* 102,
963 110-119.
- 964 Zhang, R., Sun, X.S., Shi, A.J., Huang, Y.H., Yan, J., Nie, T., Yan, X., Li, X., 2018.
965 Secondary inorganic aerosols formation during haze episodes at an urban site in
966 Beijing, China. *Atmos. Environ.* 117, 275-282.
- 967 Zhang, R.Y., Jing, J., Tao, J., Hsu, S. C., Wang, G., Cao, J., Lee, C. S. L., Zhu, L.,
968 Chen, Z., Zhao, Y., Shen, Z., 2013. Chemical characterization and source
969 apportionment of PM_{2.5} in Beijing: seasonal perspective. *Atmos. Chem. Phys.* 13,
970 7053-7074.
- 971 Zhang, Y.L., Schnelle, K.J., Abbaszade, G., Zimmermann, R., Zotter, P., Shen, R.R.,
972 Schäfer, K., Shao, L.Y, Prévôt, A.S.H., Szidat, S., 2015a. Source apportionment of
973 elemental carbon in Beijing, China: Insights from radiocarbon and organic marker
974 measurements. *Environ. Sci. Technol.* 49, 8408-8415.
- 975 Zhang, Y. L., Huang, R. J., El Haddad, I., Ho, K. F., Cao, J. J., Han, Y., Zotter, P.,
976 Bozzetti, C., Daellenbach, K. R., Canonaco, F., Slowik, J. G., Salazar, G.,
977 Schwikowski, M., Schnelle-Kreis, J., Abbaszade, G., Zimmermann, R.,
978 Baltensperger, U., Prevot, A. S. H., Szidat, S., 2015b. Fossil vs. non-fossil sources
979 of fine carbonaceous aerosols in four Chinese cities during the extreme winter haze
980 episode of 2013. *Atmos. Chem. Phys.* 15, 1299-1312.

Highlights

1. Concentrations of PM_{2.5} and components reduced significantly during the APEC period.
2. Major components in PM_{2.5} and other pollutants were comparable with other cities.
3. Vehicle restrictions could lower atmospheric NH₃ concentration over Beijing.
4. Emission control measures significantly increased ground-level O₃ concentrations.

Competing interests

The authors declare that they have no conflict of interest.

ACCEPTED MANUSCRIPT